NANOMEDICINE
https://doi.org/10.1080/17435889.2025.2550239

Taylor & Francis
Taylor & Francis Group

REVIEW

OPEN ACCESS Check for updates

Localized treatment of glioblastoma: a review of clinical strategies and advances in drug delivery systems

Cristiano Pesce[a*], Giulia Rodella[b,c*], Agnese Fragassi[a], Mariangela Garofalo[a], Stefano Salmaso[a], Paolo Caliceti[a], Bernard Gallez[c] and Alessio Malfanti[a,b]

[a]Department of Pharmaceutical and Pharmacological Sciences, University of Padova, Padova, Italy; [b]UCLouvain, Louvain Drug Research Institute, Advanced Drug Delivery and Biomaterials, Brussels, Belgium; [c]UCLouvain, Louvain Drug Research Institute, Biomedical Magnetic Resonance, Brussels, Belgium

ABSTRACT

The prognosis for glioblastoma patients remains poor despite recent advances in neurosurgery, chemotherapy, and radiotherapy. One promising treatment strategy lies in the localized delivery of therapeutics through drug delivery systems designed to enhance existing clinical treatments by directly targeting the tumor site or surrounding area. This review explores the latest advancements in localized therapies for glioblastoma, highlighting recent preclinical and clinical studies and examining how we can integrate these approaches – including stereotactic techniques such as convection-enhanced delivery and therapies targeting the post-surgical resection cavity – with drug delivery systems. We describe the features that the drug delivery system should possess for the efficient transport of drugs for both inoperable and resectable glioblastoma local treatment. Finally, this review discusses future directions that may facilitate the clinical translation of localized treatment strategies for glioblastoma.

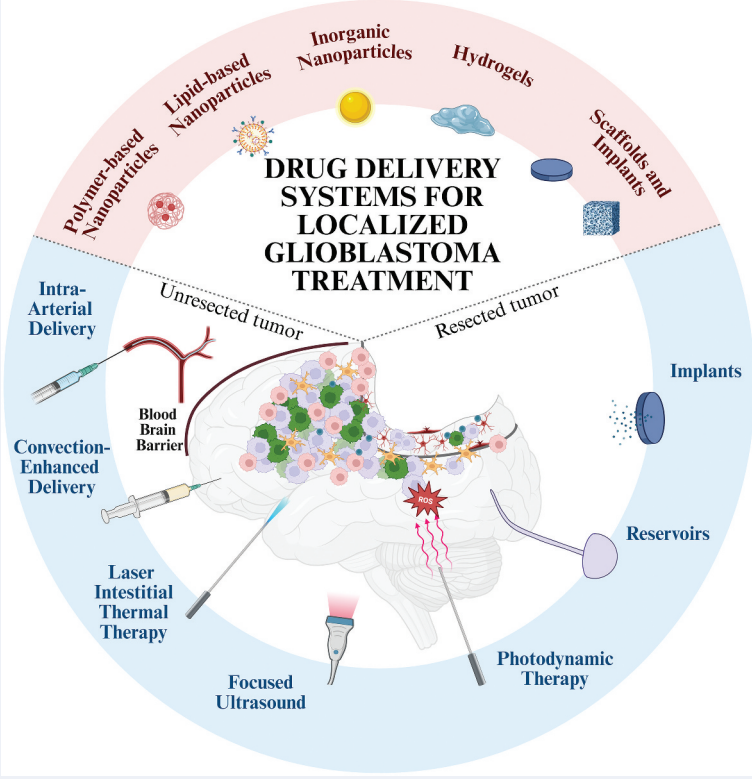

ARTICLE HISTORY
Received 21 May 2025
Accepted 18 August 2025

KEYWORDS
Glioblastoma; drug delivery; localized treatment; implants; nanomedicine; controlled drug release; neurosurgery

1. Introduction

Patients with glioblastoma (GBM) – the most aggressive and deadliest type of brain cancer – suffer from a median survival time of ~15 months and a five-year median survival rate of less than 5% [1]. Despite decades of unrelenting effort by the research and medical communities, GBM remains an unmet

CONTACT Alessio Malfanti alessio.malfanti@unipd.it Department of Pharmaceutical and Pharmacological Sciences, University of Padova, Via F. Marzolo, 5, Padova 35135, Italy; UCLouvain, Louvain Drug Research Institute, Advanced Drug Delivery and Biomaterials, Avenue Mounier 73 B1.73.12, Brussels 1200, Belgium
*Equal contribution.

This article has been corrected with minor changes. These changes do not impact the academic content of the article.

Article highlights

- Glioblastoma (GBM) is an unmet medical need.
- Approximately 60% of GBM patients receive the standard Stupp protocol after diagnosis, which has remained unchanged since 2005. This treatment includes maximal safe tumor resection, followed by radiotherapy and concurrent temozolomide (TMZ) chemotherapy; however, the median survival for GBM patients is approx. 15 months, highlighting the need to find new strategies to treat GBM.
- Locoregional treatments bypass the blood-brain barrier (BBB), allowing higher drug concentrations at the tumor site with fewer systemic side effects. This approach also enables the use of drugs that are ineffective systemically, offering new possibilities for GBM therapy.
- Various drug delivery systems (DDS) have been developed for localized GBM treatment. These DDS use biocompatible and biodegradable materials to form adaptable matrices that offer advantages over rigid implants. Design must be tailored to the tumor's characteristics, whether resected or unresected.
- For unresected GBM, effective DDS to GBM is hindered by physiological barriers such as high interstitial pressure and altered extracellular matrix composition. Nanoparticle size (~70 nm) and surface charge (neutral to slightly negative) are crucial for optimal diffusion and uptake. Additional strategies may aid penetration, but challenges like drug resistance, poor retention, GBM's heterogeneity, and immunosuppressive microenvironment must also be addressed.
- The post-surgical GBM resection cavity offers a unique environment for localized drug delivery, marked by irregular shape, fluid dynamics, and residual tumor cells. Implanting DDS here enables sustained therapeutic release, but requires precise design to ensure controlled, prolonged drug delivery within the therapeutic window. Key factors include drug loading, solubility, matrix degradation, and biocompatibility. DDS must also match brain tissue mechanics to avoid immune responses and damage to healthy tissue.

medical need. Classified by the World Health Organization (WHO) as a grade 4 astrocytoma, GBM accounts for ~ 50% of all gliomas and represents the third leading cause of cancer-related deaths [2,3]. GBM can be divided into two genetically different subcategories: i) primary GBM (~90% of cases), where the tumor arises without previous lower-grade pathology or symptoms, and ii) secondary GBM (~10% of cases), where the tumor develops via the progressive transformation of lower-grade gliomas (e.g., anaplastic astrocytoma and low-grade oligodendroglioma). These two GBM forms are morphologically identical and indistinguishable regarding clinical management and outcome. Additional GBM classifications rely on genetic and molecular profiles, including information regarding mutations in the isocitrate dehydrogenase (*IDH*), epidermal growth factor receptor (*EGFR*), tumor protein p53 (*TP53*), and Phosphatase and TENsin homolog (*PTEN*) genes [4,5]. GBM patients possess an average age at diagnosis of ~64, with higher incidence observed in male than female patients. While the US healthcare system diagnoses more than 10,000 new GBM cases each year, disease incidence varies from country to country in Europe, with age-standardized rates ranging between 3–7 cases per 100,000 individuals. In China, GBM represents 8.56% of all brain cancers, with a higher prevalence in male (60.17%) than female patients (39.83%) [6]. Notably, the United Kingdom suffers one of the highest rates of GBM diagnosis, with an age-standardized incidence rate of 7.1 per 100,000 individuals [7].

Currently, GBM treatment remains a challenge for several reasons:

(i) GBM is shielded by various inherent central nervous system barriers (i.e., the blood-cerebrospinal fluid, arachnoid, and blood-brain barriers) and the blood-tumor barrier, which represent additional challenges for the delivery of chemo-/immuno-therapeutics and the passage of immune cells into the tumor [8]

(ii) The immunosuppressive tumor immune microenvironment (TIME) enhances the resistance of GBM to radiotherapies, chemotherapies, and other emerging therapies (e.g., immunotherapies and viral therapies) by suppressing immune system recognition [9]

(iii) Highly infiltrative GBM cells impede total surgical removal without damaging surrounding neurological tissues; importantly, ~80% of cases of GBM recurrence arise inside or at the GBM margin of the radiation field and originate from GBM-associated cancer stem cells, while local recurrence associates with substantially shortened progression-free survival [10]

(iv) Tumor heterogeneity involves inter- and intra-patient variability characterized by a wide variety of signaling pathway events even within a single tumor mass; this entails significant molecular complexity and, in turn, restricts the effectiveness and availability of targeted therapies [11]

(v) Post-surgical inflammation drives GBM-associated cancer stem cell-mediated recurrence [12]

(vi) Developmental, genomic, and epigenetic features render GBM resistant to chemo-/immuno-therapeutics [13]

Unfortunately, the development of a "cure" for GBM in the near future remains an unlikely prospect; instead, efforts have focused on designing localized treatments for inoperable GBM or delaying postoperative GBM recurrence.

Locoregional methods for delivering therapeutics offer a promising strategy to overcome the previously mentioned challenges hindering successful GBM treatment. By combining drug delivery directly into the tumor or the resection cavity with existing clinical practices, these approaches hold significant potential but are often overlooked; here, the need to summarize this review work.

This review comprises three main sections. The **first** section provides a concise clinical overview of GBM treatment and progress made so far; the **second** section focuses on strategies for the localized treatment of GBM; and the **third** section explores how drug delivery systems (DDSs) for both unresected and resected GBM can support the above-described treatment approaches through clinically relevant therapeutic strategies. After these main sections, we review high-impact studies demonstrating strong translational potential as proof of concept and present future perspectives to advance the clinical translation of GBM treatment strategies.

2. Clinically approved treatments for glioblastoma

2.1. The standard of care for glioblastoma: the Stupp protocol

Around 60% of GBM patients undergo the standard of care – the Stupp protocol – after diagnosis. The Stupp protocol –

which has remained unchanged since 2005 - involves the maximal safe surgical resection of the accessible tumor, followed by concurrent radiotherapy (RT; 60 Gy in 30 fractions) and chemotherapy with temozolomide (TMZ; 75 mg/m^2/day for six weeks) and six maintenance cycles of TMZ (150–200 mg/m^2/day) [14–16]. The following sections will analyze the distinct components of this protocol.

2.1.1. Neurosurgery

Surgery represents the cornerstone option in the standard of care for GBM. Magnetic resonance imaging (MRI) and diffusion tensor imaging map critical brain areas and white matter tracts to identify eloquent brain regions (those critical for cognitive functions) and minimize neurological deficits [17]. Maximal safe resection – the primary surgical goal – correlates with improved survival and relief of symptoms. While strong prognostic factors remain essentially patient-related, the extent of resection represents the most important treatment-related predictor. A higher extent of resection associates with longer life expectancy, with the most extended survival observed in those patients undergoing gross total resection followed by RT and TMZ treatment [18]. Surgery via craniotomy can be tailored according to GBM location. Fluorescence-guided surgery with 5-aminolevulinic acid (5-ALA) enhances visualization of tumor margins, leading to higher resection rates and improved median survival rates [19]. For tumors located in eloquent brain regions, awake craniotomy or intraoperative electrical stimulation mapping can maximize the extent of resection and preserve neurological functions [20,21]. Preoperative conditions such as corticosteroid and antiepileptic drug treatment have also been considered. Steroids (i.e., dexamethasone and methylprednisolone) can control cerebral edema and signs of intracranial hypertension, thus improving surgical resection [22]; however, current evidence does not strongly support the routine use of prophylactic antiepileptic drugs for patients undergoing brain surgery [23].

2.1.2. Radiotherapy (RT)

RT targets residual GBM cells after surgery to slow tumor progression. Fractionated external beam radiation therapy – daily fractions of external beam radiation in the area surrounding GBM at 2 Gy five times per week (60 Gy over six weeks) – represents the standard treatment approach [24,25]. Fractionating doses allow healthy brain tissue to repair itself during the time between each dose, minimizing side effects while maximizing damage to cancer cells, which repair DNA damage less efficiently [25]. The maximal advantage of RT use occurs when combined with surgical resection and TMZ treatment. Stereotactic radiosurgery – a more focused strategy that delivers higher doses of radiation to a precise tumor area – represents an improvement over traditional RT and the preferred approach for the localized treatment of small GBM tumors or well-defined recurrences [26]. Adverse side effects of RT – commonly categorized as acute, early-delayed, or late-delayed – are based on the onset of symptoms [27]. Acute encephalopathy can occur within hours to weeks after RT and exacerbates neurological deficits such as nausea, vomiting, headache, and confusion [27]. Acute side effects can lead to herniation and death in patients with large tumors; however, these side effects remain treatable. A high radiation dose per fraction (> 20 Gy) represents the primary risk factor for the development of acute encephalopathy [28].

2.1.3. Temozolomide (TMZ)

Patients receive treatment involving daily oral TMZ (75 mg/m^2) during RT and six cycles of TMZ (150–200 mg/m^2) as adjuvant therapy for five days during each 28-day cycle after RT [15]. TMZ – an oral chemotherapeutic drug – alkylates DNA at the O^6 position of guanine residue, creating DNA damage that leads to tumor cell apoptosis. Unfortunately, GBM cells can quickly develop TMZ resistance, mainly via the upregulation of O^6-methylguanine-DNA methyltransferase (MGMT), a DNA repair enzyme that removes the methyl group from O^6-guanine to support DNA replication, overcoming the DNA damage induced by TMZ and thus reducing cancer cell sensitivity to this drug [29,30]. Under conditions of TMZ treatment, MGMT can remove the methyl group in O^6-methylguanine thereby neutralizing the TMZ-induced DNA damage and reducing the efficacy of the drug [31]. This effect is more pronounced in unmethylated tumors (with increased MGMT activity) that commonly exhibit superior resistance to TMZ than methylated GBM [31]. TMZ exhibits linear pharmacokinetics and high bioavailability, penetrates the cerebrospinal fluid effectively, and does not rely on hepatic metabolism for activation [32]. In addition, despite glioblastoma stem-like cells (GSCs) make up as little as 1% of the total cells in a GBM tumor, they play a key role in resistance to TMZ. This is due to their capacity to regenerate tumor heterogeneity, which in turn fosters resistance to both conventional chemotherapeutic agents and targeted treatments [33]. Recently, it has been proposed that TMZ can promote GSC differentiation [34]. Adverse effects associated with TMZ include hematologic toxicity, with thrombocytopenia affecting 10–20% of patients. Less common non-hematologic toxicities associated with TMZ include nausea, anorexia, fatigue, and hepatotoxicity; significantly, TMZ suppresses immune responses, which limits the use of immunotherapy in the standard of care [35]. Of note, TMZ does not provide any benefit beyond that observed from RT treatment in IDH wildtype (wt) GBM [36].

2.2. Additional approved treatments for glioblastoma

2.2.1. Gliadel wafers

Developed in the early 1990s, Gliadel wafers were designed to overcome the impermeability of the blood-brain barrier to drugs to support localized GBM treatment. Each Gliadel wafer is impregnated with the alkylating agent carmustine (1,3-bis(2-chloroethyl)-1-nitrosourea; BCNU) [37], has a cylindrical shape (14.5 mm diameter, 1 mm thickness), and weighs ~200 mg (7.7 mg BCNU). Given a recommended dose of 61.6 mg BCNU for GBM patients, around eight wafers can be placed into the resection cavity during surgery to circumvent the blood-brain barrier and achieve high local drug concentrations within the brain. Gliadel wafers comprise a biodegradable random copolymer (polifeprosan 20) formed of 1,3-bis-(p-carboxyphenoxy)propane and sebacic acid monomers at a 20:80 molar ratio conjugated by anhydride bonds

that erode over time to release BCNU into the surrounding tissue [38,39]. The advantages of Gliadel wafers relate to the constant release rate of BCNU over a week; however, convective transport due to the interstitial flow resulting from edema augments diffusion in the days immediately following surgery. Gliadel wafers biodegrade over three weeks, although polymer traces have been found 13–23 weeks post-implantation in select patients [40–42]. Studies of Gliadel wafers have demonstrated overall safety (i.e., low systemic toxicities and prolonged overall survival compared to patients treated with placebo wafers) and increased benefit when combined with RT and TMZ (NCT02684838); however, the European Association of Neuro-Oncology guidelines for GBM treatment does not include Gliadel wafers due to inefficacy in providing survival benefits and their use in clinical practice remains limited [41].

2.2.2. Bevacizumab

The status of GBM as one of the most vascularized tumors makes anti-angiogenic therapeutic strategies for GBM an attractive option. In 2009, the U.S. Food and Drug Administration (FDA) approved bevacizumab – a monoclonal antibody that binds to circulating vascular endothelial growth factor (VEGF) and inhibits biological activity by preventing interactions with its receptor – for the first-line treatment of recurrent GBM [43,44]. Blocking VEGF signaling and the associated reduction in angiogenesis leads to limited blood vessel formation and nutrient/oxygen supply to the tumor, thereby slowing tumor growth [45]. While not impacting overall survival, bevacizumab treatment improves progression-free survival and recent strategies have explored extending the median survival rate of GBM patients by implementing bevacizumab in the standard of care. Bevacizumab treatment also reduces peritumoral edema, often improving neurological symptoms and quality of life in specific GBM patient subcategories [46].

2.2.3. Tumor-treating field (TTFields)

In 2015, the FDA approved the use of tumor-treating fields (TTFields; commercially known as Optune®) – a noninvasive portable medical device with transducer arrays placed directly on the patient's scalp that produces low-intensity, intermediate-frequency electric fields targeted to the GBM site [47,48]. TTFields disrupt cancer cell division by altering microtubule formation and causing the abnormal alignment of intracellular organelles, leading to cell cycle arrest and cancer cell apoptosis [49]. Several trials have established the clinical benefits of TTFields combined with the standard of care; this included the EF-14 trial (NCT00916409), where patients treated with TTFields and TMZ demonstrated a significant improvement in survival compared to those treated with TMZ only [48,50]. Owing to the localized mechanism of action and the general absence of systemic adverse effects, TFFields represent a strategy that should be explored for novel combination therapies in addition to the standard of care [51].

3. Localized treatment strategies for glioblastoma

Despite the TMZ's ability to cross the BBB, only a small fraction of orally administered drug reaches the tumor site, significantly limiting its therapeutic efficacy [52]. Consequently, localized treatments have emerged as the most straightforward and promising strategy to address the challenges associated with GBM management [41]; this approach overcomes the barriers associated with systemic delivery, bypassing the BBB and achieving higher drug concentrations at the tumor site with low systemic side effects [53]. Most importantly, localized treatments enable the application and repurposing of many molecules that cannot be applied systemically (alone or combined), thereby opening new perspectives in treating this unmet medical need [54]. This section discusses preclinical and clinical localized therapeutic strategies for GBM treatment, emphasizing their potential to augment the current standard of care (Figure 1).

3.1. Intra-arterial delivery (IAD)

Intra-arterial delivery (IAD) involves administering high doses of free therapeutics (e.g., small drugs, antibodies, and oncolytic viruses) and DDSs directly to the GBM tumor bed via an intra-arterial catheter. This approach takes advantage of GBM's extensive capillary network and peritumoral vasculature, limiting the volume of distribution to a targeted vascular region; overall, drugs diffuse into the tumor and do not enter circulation [55]. Maximizing IAD often entails the added implementation of transient blood-brain barrier disruption with osmotic agents such as mannitol, which enhance drug passage into the brain [56,57]; indeed, osmotic disruption can increase the levels of chemotherapeutics in the brain by up to 90-fold [58]. Although interest in IAD has decreased with the advent of advanced neurosurgical techniques, the selective IAD of RT and TMZ with transient blood-brain barrier opening remains a promising strategy, especially for patients who cannot undergo surgery [53].

3.2. Convection-enhanced delivery (CED)

Convection-enhanced delivery (CED) involves directly injecting therapeutics into the brain parenchyma or tumor tissue [59]. While primarily used for delivering chemotherapeutics, CED can introduce monoclonal antibodies, targeted toxins, proteins, viruses, and DDSs into the tumor at preclinically-/clinically-relevant levels [60]. CED establishes a positive pressure gradient that allows uniform drug distribution up to 2–3 cm, thereby improving the spatial distribution of therapeutics that typically diffuse poorly (regardless of their molecular weight and hydrophobicity) [60]. Infusion parameters such as drug concentration, volume, flow rate, and duration require careful adjustment to optimize treatment efficacy and avoid unwanted side effects. Although CED can be applied to patients with inoperable or recurrent tumors, enabling the distribution of large volumes of drugs at high concentrations while minimizing systemic toxicity, this approach has seen more pronounced success in laboratories than in clinical settings [41,53].

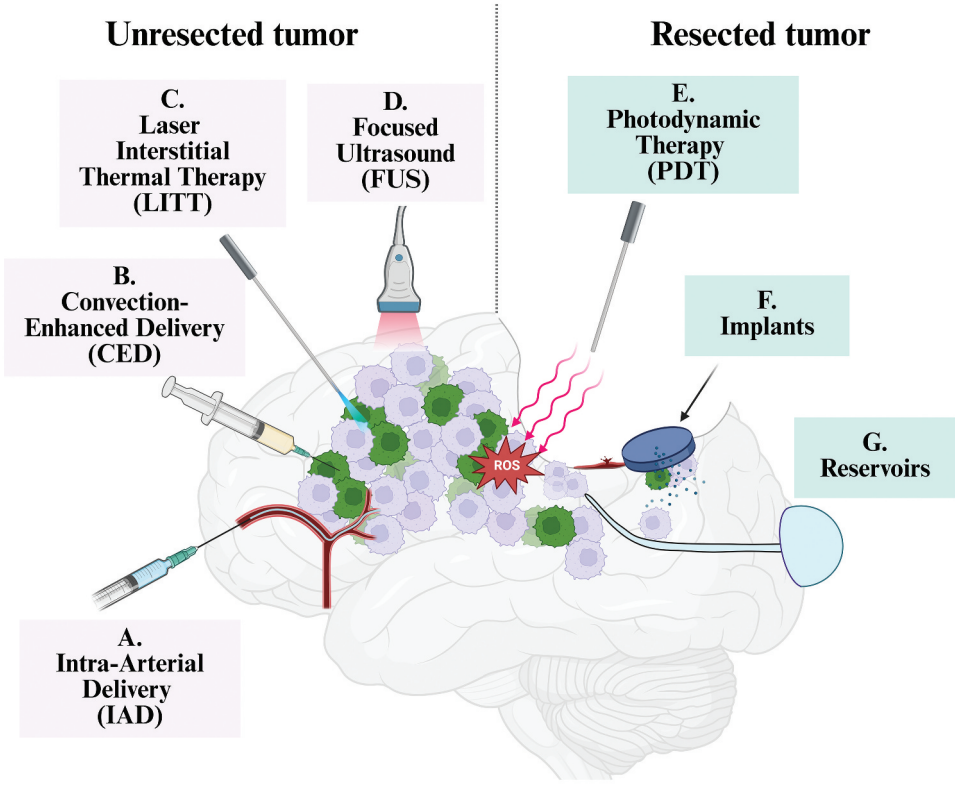

Figure 1. Localized treatment for unresected and resected glioblastoma. *unresected tumor treatments*: A. Intra-arterial delivery (IAD) relies on administering nanomedicines to the tumor via intra-arterial catheters. B. Convection-enhanced delivery (CED) involves the direct injection of therapeutics into the tumor tissue by establishing a positive pressure that allows selective distribution. C. Laser interstitial thermal therapy (LITT) employs laser-mediated tissue heating. D. Focused ultrasound (FUS) comprises the transcranial delivery of ultrasound waves to focal volumes. *resected tumor treatments*: E. Photodynamic therapy (PDT) employs photosensitizers that generate reactive oxygen species when activated by visible light, which disrupts cancer cell metabolism. The placement of (F) implants and (G) reservoirs in the resected cavity or under the skin supports the long-term delivery of therapeutics. Cancer cells are represented in purple; green cells represent generic cells of the TIME. Created in https://biorender.com.

Several factors that hamper the clinical application of CED in GBM patients must be addressed: i) the heterogeneous nature of GBM, with varying degrees of necrosis, angiogenesis, and metabolic rates (even within the same tumor) that prompt widely differing rates of clearance after injection; ii) catheter design, which limits diffusion of therapeutics into the GBM stroma and the need of DDSs designed for higher penetration, and iii) a lack of training, with neurosurgeons often not placing the catheter in the correct position, thus limiting the potential of this technique [53,61]. Despite the limits, several clinical trials are currently exploring CED's potential for localized GBM treatment.

3.3. Laser interstitial thermal therapy (LITT)

Laser interstitial thermal therapy (LITT; also known as stereotactic laser ablation) relies on the implantation of an optical fiber into the tumor through a burr hole. This approach supports tumor heating to 42.5–45.5°C using a laser with a wavelength between 1,070–980 nm [62,63] and temperature monitoring in real-time using an intraoperative MRI thermometer. In general, patients tolerate LITT well, although a small patient population experiences adverse side effects such as seizures [64]. LITT represents a promising treatment approach for patients with GBM tumor volumes of less than 10 cm^3 (corresponding to a radius of 1.33 cm), inoperable GBM, or poor functional status and has advantages such as cost-effectiveness [64]. Of note, descriptions of LITT´s effectiveness have provided contradictory outcomes. Clinical studies have reported that LITT extended survival (median: 9.0–11.2 months) in patients with recurrent GBM refractory to other treatments [65]; however, a study of 24 LITT-treated patients reported that they experienced permanent neurological symptoms [66]. Similarly, 15.5% of 54 patients treated with LITT for primary or recurrent GBM developed serious adverse events (e.g., edema, seizures, and hydrocephalus) without any accompanying improvements in overall survival [67]. Considering these results, we may require additional data to fully assess the efficacy of LITT, possibly in combination with other strategies.

3.4. Focused ultrasound (FUS)

Focused ultrasound (FUS) – an emerging technology for the localized treatment of various neurological diseases – allows the transcranial delivery of ultrasound waves to focal volumes in GBM, offering a noninvasive and precisely targeted therapeutic option [68]. FUS allows the transient opening of the blood-brain barrier to improve the delivery of therapeutics that typically display poor or precluded passage [69]. The first clinical trial of FUS for GBM in 15 patients provided only a limited perspective due to the obsolete equipment

employed [70]; however, since the time of this trial (1991), more advanced technologies have been developed, opening new possibilities for the inclusion of FUS in GBM management. We direct the reader to the review of Young et al. for additional information on this approach [71].

3.5. Photodynamic therapy (PDT)

Photodynamic therapy (PDT) involves the use of photosensitizing agents activated by visible light and oxygen within tissues to generate highly cytotoxic oxygen singlets ($^1O_2$) and other reactive oxygen species (ROS). ROS disrupts cancer cell metabolism and prompts their elimination [72]. GBM treatment via PDT involves implanting laser-emitting lights (630–-690 nm) in the resected cavity. Besides eliminating cancer cells via ROS production, PDT destroys the microvasculature and triggers an immune response to induce immunogenic cell death [73]. PDT treatment for GBM currently involves two main photosensitizing molecules: 5-ALA, commonly used by neurosurgeons to detect GBM margins; and Photofrin, which has FDA approval [74,75]. Primary concerns regarding the use of PDT relate to the lack of laser penetration into the tissue, as biological tissues tend to absorb and scatter light, thereby limiting the penetration depth of visible and ultraviolet light. The maximum penetration achievable (5 mm, with some effects observed up to 9 mm) remains insufficient to reach highly infiltrative GBM cells [76]; however, the limited current clinical use of 5-ALA, the implementation of the standard of care, and the low-risk nature of this therapy warrant further studies [76].

3.6. Implants and reservoirs

Implants and drug reservoirs placed into the GBM resected cavity have become a preferred strategy for post-surgical localized drug delivery following the success of Gliadel wafers [53]. The concept of implantable biomaterials (e.g., wafers, films, disks, and rods) has been explored for GBM treatment since the late 1960s [77]; for example, Ommaya or Rickham reservoirs use catheters connected to needle-based implants linked to a subdermal implant [78]. These reservoirs can be accessed intermittently, offering greater flexibility for patients and clinicians during treatment. While wafers and reservoirs support the long-term delivery of therapeutics, prolonged brain exposure to the external environment through these reservoirs can lead to side effects such as inflammation and infection [41]. Although the device's small size (around the size of a quarter) minimizes patient discomfort, individuals with reservoirs may still experience challenges in their daily lives due to the permanent presence of the external device [79]. Modifying drug compounds, dosage, and implantation techniques could potentially enhance the efficacy and safety of implants and reservoirs [41].

4. Drug delivery systems for the localized treatment of glioblastoma

Over the past few decades, DDSs with different designs, compositions, shapes, dimensions, and architectures have been developed for the localized treatment of GBM [41,80]. Said DDSs include hydrogels, polymer-drug conjugates, nanoparticles (NPs), fibers, and meshes. The biomaterials employed for implantable DDSs typically include biocompatible and biodegradable polymers, lipids, or inorganic compounds [81,82] that form a soft matrix or hydrogel that offer mechanical benefits over rigid implants, which often lack adaptability and on-site stability. According to the physico-chemical properties of the biomaterial, drug release is either controlled by i) diffusion of DDSs into the GBM stroma followed by release after cell internalization or ii) the biodegradation (erosion) of the DDS matrix. These approaches support access into deeper GBM sites and sustained drug release; however, each approach must be rationally designed/tuned according to the tumor type or form (unresected or resected) [80,82]. The following sections briefly introduce the distinct types of DDSs employed for the localized treatment of unresected and resected GBM.

4.1. Drug delivery systems for unresected glioblastoma

4.1.1. Key approaches for designing drug delivery systems for unresected glioblastoma

Physiologically, brain tumors and normal tissue present challenges for effective drug delivery. Increased extracellular space, tortuosity, and dense cellular patterns create significant barriers to drug and particle diffusion through GBM tumors [83]. Furthermore, GBM tumors suffer from high interstitial fluid pressure, which can hinder the uptake of various therapeutics [84], while tumor-associated alterations in extracellular matrix composition, volume, and structure can impair diffusion [85]; therefore, accounting for these tumor-specific barriers remains essential to the design of optimally behaving DDSs. From the perspective of a nanoparticle, size significantly influences distribution within the brain – particles of ~70 nm possesses a better ability to navigate through the extracellular matrix. Additionally, the surface charge of nanoparticles plays a crucial role in cell uptake and biocompatibility – neutral or slightly negative charges minimize nonspecific interaction with cerebrospinal fluid and GBM tumor cell membranes [86,87]. Moreover, specific strategies, including the co-delivery of enzymes or osmotic agents, may help improve penetration, although their clinical utility remains uncertain [88]. Overcoming the blood-brain barrier may not represent the only requirement, as additional challenges (e.g., drug resistance, poor retention, and limited cellular uptake) must also come into consideration. In addition, it should consider that GBM is characterized by intratumoral and intertumoral heterogeneity (which makes each tumor unique) and an immunosuppressive TIME that promote GBM growth via complex interactions with the healthy brain [89,90] (Figure 2).

To address these challenges, the following sections will explore the potential use of various DDS types for the localized treatment of GBM designed to overcome multifaceted barriers.

4.1.2. Polymer-based nanoparticles

Polymer-based nanoparticles have tremendous potential when considering drug delivery to brain tumors such as GBM, as they enhance diffusion and penetration in the brain,

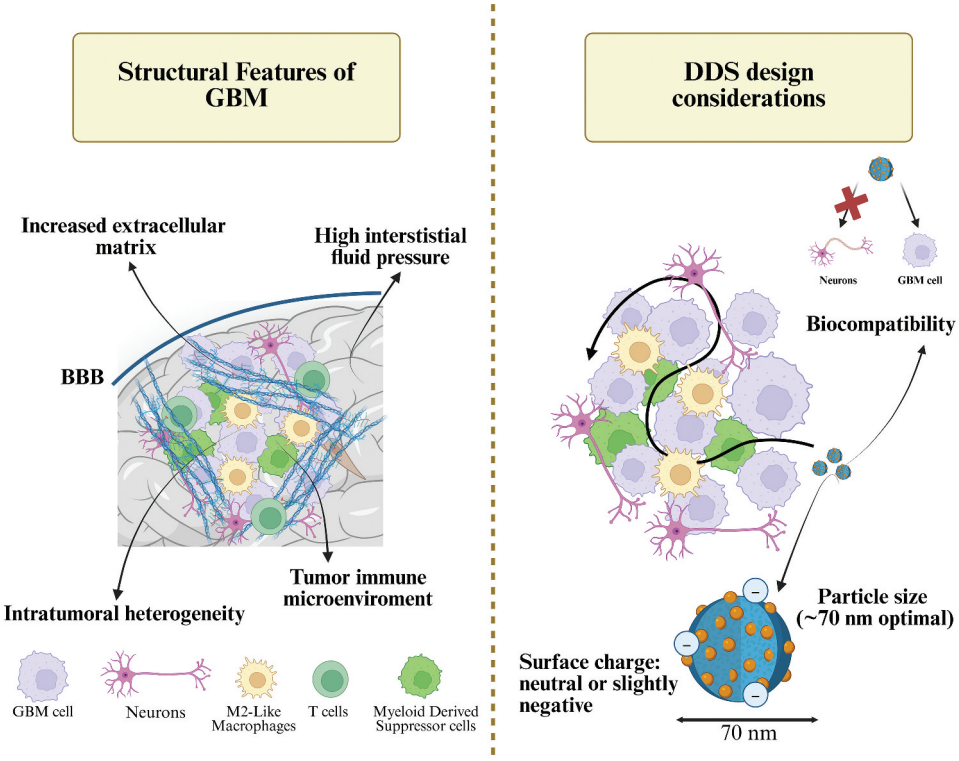

Figure 2. Challenges and design considerations for local drug delivery in unresected GBM. The design of drug delivery systems for unresected glioblastoma (GBM) should address specific challenges, including biocompatibility, drug resistance, and poor drug distribution and retention into the tumor. The different features of brain tumors (e.g., increased extracellular space, tortuosity, dense cellular patterns, high interstitial pressure, and alterations in the extracellular matrix, as well as the role of the tumor immune microenvironment) must be considered for efficient cell uptake and distribution in the brain. Created in https://BioRender.com.

improve tumor cell uptake, and increase drug accumulation at the tumor site. The encapsulation of drugs within nanoparticles protects drugs from degradation, reduces toxicity, provides sustained release, and improves tissue retention. This section reviews those studies showcasing the effectiveness of polymeric nanoparticles in delivering anticancer drugs and nucleic acid therapeutics, highlighting their potential to enhance treatment outcomes for brain tumors (Table 1).

Poly(lactic-co-glycolic acid) (PLGA) and polyethylene glycol (PEG) represent prominent examples of materials employed in polymer-based DDSs due to their beneficial properties. PLGA nanoparticles have been extensively studied for the CED of chemotherapeutic drugs such as paclitaxel (PTX) [91,92], docetaxel (DTX), irinotecan (IRT) [93], camptothecin [94], carboplatin [95], and mitoxantrone [96]. While PLGA-based nanoformulations of drugs display superior efficacy to free drugs, coating PLGA nanoparticles with PEG reduces adhesion to cell membranes, potentially enhancing brain penetration. For instance, Hanes et al. loaded PTX into PLGA-co-PEG block copolymer nanoparticles of 70 nm in diameter and demonstrated that these nanoparticles diffused 100 times faster than similarly sized PTX-loaded PLGA nanoparticles not containing PEG [91,92]. The densely PEGylated PTX-loaded PLGA nanoparticles significantly inhibited tumor growth after CED administration to a rat gliosarcoma model (9 L) compared to non-PEGylated PTX-loaded PLGA nanoparticles or free PTX.

Similarly, Mastorakos et al. created a densely PEGylated nanoparticle composed of polyethyleneimine (PEI), a cationic molecule widely used as a non-viral gene vector [97]. The engineered gene vectors rapidly diffused throughout the brain parenchyma, displaying significantly enhanced vector distribution and transgene expression in vivo compared to previously published platforms. Another study from Mastorakos et al. reported comparable results with PEGylated poly(β-amino ester)-plasmid (p)DNA nanocomplexes; although spherical, these nanoparticles became homogeneously distributed throughout the rodent striatum and mediated widespread, high-level transgene expression [98]. Compared to the non-PEGylated formulation, these PEGylated poly(β-amino ester)-pDNA nanocomplexes provided two-fold higher overall in vivo gene expression, most likely due to improved brain distribution.

More interestingly, Saltzmann and colleagues explored the impact of nanoparticle decoration on cellular tropism in the context of the brain/GBM tumor cell microenvironment [86] (Figure 3). Polylactic acid (PLA)-based nanoparticles with differing surface chemistries administered into the rat brain via CED revealed that modification with "stealth" surface molecules (PEG, forming PLA-PEG nanoparticles) and hyperbranched glycerol (HPG, forming PLA-HPG nanoparticles) inhibited nanoparticle internalization by all cell types, including tumor cells; however, they reestablished and enhanced brain penetration by adding bio-adhesive aldehyde end groups (CHO, PLA-HPG-CHO nanoparticles). The therapeutic assessment of the different nanoparticle formulations loaded with the potent cytotoxic agent Epothilone B (EB, 0.1 mg/kg) in an orthotopic rat GBM RG2 model highlighted the importance of balancing efficient cellular uptake and minimizing toxicity to healthy tissues. Treatment with EB-loaded PLA-PEG nanoparticles induced a modest improvement in survival

Table 1. Relevant examples of preclinical drug delivery systems for unresected glioblastoma.

Nanocarrier	Delivery Route	Drug	Dose	Glioblastoma Model	Outcome	Reference
Polymer-based Nanoparticles						
PLGA-PEG	CED	PTX	2.5 mg/kg	Orthotopic rat 9 L model	**Tumor Growth**: Rats treated with PLGA-PEG NP showed a superior control of the tumor growth compared to PLGA NPs and untreated	[92]
PBAE-PEG	CED	DNA	10 µg	Healthy rat brain	**Local distribution**: PBAE-PEG complexes showed superiror diffusion than non-PEGylated complexes	[98]
PLA PLA-PEG PLA-HPG PLA-HPG-CHO	CED	EB	0.1 mg/kg	Orthotopic rat RG2 model	**Survival**: Saline: 16 days Free EB: 18 days PLA: 33 days PLA-PEG: 21.5 days PLA-HPG: 28 days PLA-HPG-CHO: 28 days	[86]
PLGA-PEG L-histidine	CED	DTX	2 µg	Orthotopic mouse U87MG model	**Survival**: Untreated: 30 days Free DTX: 38 days DTX-NPs: 33.5 days DTX-H-NPs: 46.5 days	[99]
Pr-DEX	CED	miRNA-145 (tumor suppressor)	Not Disclosed	3D spheroid models of human GBM cell lines (U87MG, GIN-8, GIN-28, GCE-28) Zebrafish embryos	**Cytotoxicity in spheroids**: Pr-DEX nanoparticles do not show toxicity and provide silencing of target genes **Survival**: Pr-DEX nanoparticles did not affect the survival of zebrafish embryos even at the highest concentration and incubation time	[100]
PAA-PEG	CED	Cisplatin	12 µg	Orthotopic rat F98 gliosarcoma model	**Survival**: Saline: 28 days Free cisplatin: 12 days Non-PEGylated PAA- cisplatin conjugates: 40 days PEGylated PAA-cisplatin conjugates: 80% of animals survived the study (100 days)	[103]
DEX PEG PAMAM Dual-sensitive linker	CED	DOX	15 µg	Orthotopic mouse GL261-luc model	**Survival**: Untreated: 18 days, Free DOX: 21 days, Dend-NPs: 22 days, Dual-NPs: 30 days	[104]
HA-drug conjugates	CED	DOX + CpG	DOX (5 µg) CpG (10 µg)	GL261 cell line Orthotopic mouse GL261 model	**Survival**: Untreated: 27 days Free DOX/CpG: 27 days HA-DOX + free CpG: 31 days Free DOX + HA-CpG: 30.5 days HA-DOX + HA-CpG: N/A – 67% of animals survived the study period of 100 days	[105]
HA-drug conjugates	CED	DOX + GEM	DOX (5 µg) GEM (2.42 µg)	Orthotopic mouse GL261 and SB28 models	**Survival**: Untreated: 25 days DOX + GEM: 28 days HA-DOX + HA-GEM: 32 days	[107]
HA-MSA2 conjugate	CED	MSA2	5 µg	Orthotopic mouse SB28 model	**Survival**: Untreated: 19 days Free MSA2: 20 days HA-MSA2: 25 days	[108]

(*Continued*)

Table 1. (Continued).

Nanocarrier	Delivery Route	Drug	Dose	Glioblastoma Model	Outcome	Reference
mPEG-b-p(HPMAm-Bz) micelles	Subcutaneous/ Intravenous + FUS	VAL + PAN	6 mg/kg	Subcutaneous Mouse GL261 and Orthotopic Mouse HSJD-DIPG-007 GBM patient-derived Models	**Tumor growth**: **GL261**: treatment with double drug-loaded micelles decreased tumor volume by more than three-fold compared to controls **HSJD-DIPG-007**: treatment with double drug-loaded micelles combined with FUS slowed tumor growth compared to treatment with free drugs combined with FUS	[109]
Lipid-based Nanoparticles						
LNCs Chitosan	CED	PTX + CpG	Not disclosed	GL261 cell line Orthotopic mouse GL261 model	**Survival**: Saline: 28 days Free PTX: 28 days Empty LNCs: 27 days PTX-LNCs: 31 days PTX-LNCs + CpG 31 days M-LNCs: 34 days	[111]
sHDL DMPC POPC	CED + RT	DTX + CpG	0.5 mg/kg DTX CpG (Not disclosed) RT (2 Gy)	Orthotopic mouse GL261 model	**Survival**: Saline: 28 days RT: 43 days DTX-sHDL-CpG: 55 days DTX-sHDL-CpG + RT: median survival not reached	[112]
sHDL DMPC POPC	CED + RT	GW3965 + CpG	0.5 mg/kg GW3965 CpG (Not disclosed) RT (2 Gy)	GL261 cell line Orthotopic mouse GL261 model	**Survival**: Saline: 28 days RT: 34 days GW3965: 34 days GW3965-sHDL-CpG: 33 days GW3965 + RT: 35 days GW3965-sHDL-CpG + RT: median survival not reached	[113]
Dlin-MC3-DMA DSPC Chol DSPE-PEG-NH_2 HA	CED	siRNA encoding PLK1	Two injections: 0.5 mg/kg at days 20 and 22 after tumor inoculation	GBM Cell Line GBM Patient-derived neurospheres Orthotopic mouse U87MG model	**Survival**: Saline: 33 days HA-LNPs-siLuc: 34.5 days HA-LNPs-siPLK1: N/A – 60% of animals survived the study period of 95 days	[115]
DOTAP DOPE pSar	Intracranial injection	mRNA encoding GFP	150 pg	Tg(mpeg1:RFP) Zebrafish model	**Transfection efficiency**: C14-pSar2k (lipopolymer content of 2.5%-5.0%) effectively transfected cells and prompted stable *GFP* expression in the central nervous system.	[116]
DSPC DOPC Chol DSPE-PEG DOTAP	CED	DOX	40 µg	Orthotopic Rate 9 L-2Model	**Biodistribution**: DOX-liposomes well distributed throughout the tumor mass (almost covering entirely) compared to free-DOX (poor tissue distribution)	[117]
DSPC Chol DSPE-PEG	CED	TPT	10 µg/treatment	Intracranial xenograft rat U87MG or U251MG Models	**Survival**: **U87MG model**: Fluorescent liposomes (CED at day 7* – 0%) Free TPT (CED at day 7* – 0%) TPT-liposomes (CED at day 7* – 86%) Fluorescent liposomes (CED at day 12* – 0%) TPT-liposomes (CED at day 12* – 17%) **U251MG model**: Fluorescent liposomes (CED at day 14* – 0%) TPT-liposomes (CED at day 14* – 17%)	[118]

(*Continued*)

Table 1. (Continued).

Nanocarrier	Delivery Route	Drug	Dose	Glioblastoma Model	Outcome	Reference
DMPC DOTAP Chol DSPE-PEG	IAD	–	–	Orthotopic Rat C6 Glioma Model	**Biodistribution**: Large and cationic liposomes display better accumulation in GBM	[120]
Inorganic Nanoparticles						
SiO_2 BTDS Cu_2–xSe-PEG	CED + FUS	DOX	5 mg/kg	Orthotopic mouse U87MG model	**Survival**: FUS: 24 days Free DOX: 32 days Free DOX/FUS: 42 days DOX-HCu: 35 days DOX-HCu/FUS: 52 days	[123]
$SrBi_2Ta_2O_9$ DSPE-PEG_{2000}-Transferrin	CED + FUS	–	SBTO nanoparticles (3 mg/kg every five days) FUS (Not disclosed)	U87MG cell line Orthotopic mouse U87MG model	**Survival**: SBTO nanoparticles + FUS: 67%	[124]

Abbreviations: BTDS: Bis(3-triethoxysilylproyl)disulfide; CED: Convection Enhanced Delivery; CHO: Bio-adhesive aldehyde end group; Chol: Cholesterol; CpG: short single-stranded synthetic DNA molecules containing a CTP followed by a GTP; Dend: Dendrimer; Dlin-MC3-DMA: 4-(dimethylamino)-butanoic acid, (10Z,13Z)-1-(9Z,12Z)-9,12-octadecadien-1-yl-10,13-nonadecadien-1-yl ester; DMPC: 1,2-dimyristoyl-sn-glycero-3-phosphocholine; DOPC: 1,2-Dioleoyl-sn-glycero-3-phosphocholine; DOPE: dioleoylphosphatidylethanolamine; DOTAP: 1,2-dioleoyl-3-trimethylammonium-propane; DOX: Doxorubicin; DSPC: 1,2-distearoyl-sn-glycero-3-phosphocholine; DSPE: 1,2-distearoyl-sn-glycero-3-phosphoethanolamine; DTX: Docetaxel; DEX: Dextran; EB: Epothilone B; FUS: Focused Ultrasound; GEM: Gemcitabine; GFP: Green fluorescent protein; GW396: Liver-X-Receptor agonist; -H-: L-histidine; HA: Hyaluronic acid; HPG: hyperbranched glycerol; IAD: Intra-arterial delivery; LNCs: Lipid Nanocapsules; miRNA: MicroRNA; M-LNCs; multifunctional LNCs; mPEG-b-p(HPMAm-Bz): Methoxy poly (ethylene glycol)-b-(N-(2-benzoyloxypropyl) methacrylamide); mRNA: Messenger RNA; MSA2: Non-nucleotide STING agonist; NPs: Nanoparticles; PAA: Poly(aspartic acid); PBAE: poly(β-amino esters); PAMAM: Poly(amidoamine); PAN: Panobinostat; PEG: Polyethylene glycol; PLA: Polylactic acid; PLGA: Poly(lactic-co-glycolic acid); PLK1: Polo-like kinase 1 gene; POPC: 1-palmitoyl-2-oleoyl-glycero-3-phosphocholine; Pr: Protamine; pSar: polysarcosine; PTX: Paclitaxel; RT: Radiotherapy; SBTO: Piezoelectric SrBi2Ta2O9; SiO2; Silicon Dioxide; siRNA; Short interfering RNA; sHDL: Synthetic high-density lipoprotein; TPT: Topotecan; VAL: Valrubicin. *CED infusion of free drug or nanoparticles evaluated at different timings after tumor implantation – 7, 12, and 14 days.

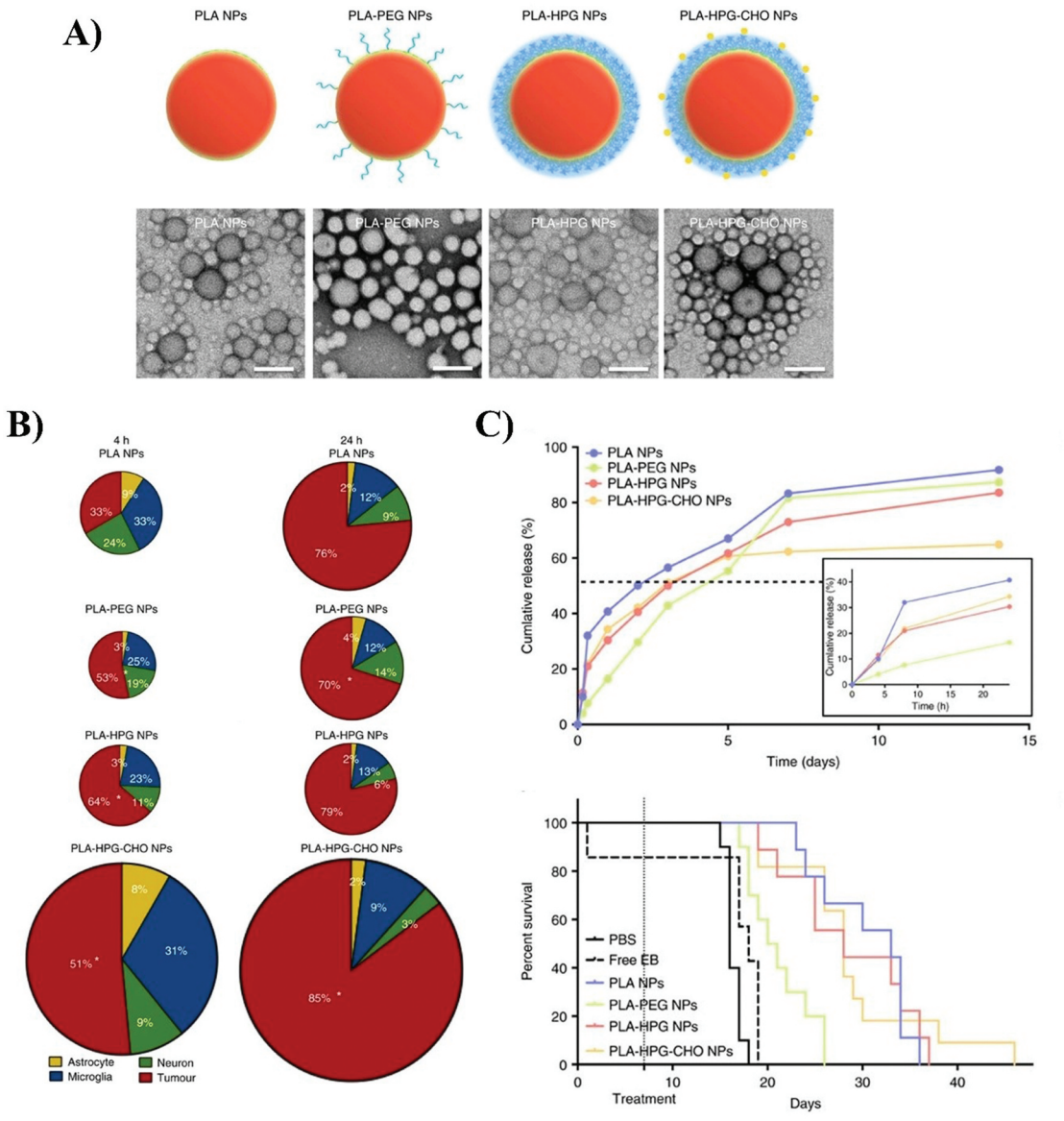

Figure 3. Nanoparticle surface properties impact cellular tropism in glioblastoma. (A) Schematic representation of polylactic acid (PLA)-based nanoparticles (NPs) with different coatings (polyethylene glycol [PEG], hyperbranched glycerol [HPG], and a bio-adhesive aldehyde end group [CHO]) (*upper images*) and particle morphology via transmission electron microscopy imaging (*lower images*). (B) Pie charts representing total PLA-based nanoparticle uptake by astrocytes, neurons, microglia, and tumor cells after 4 and 24 h. Adding CHO enhanced cell internalization compared to nanoparticles modified with PEG and HPG. (C) Surface modifications did not affect drug release *in vivo* after convection-enhanced delivery, and PLA and PLA-HPG-CHO nanoparticle treatment significantly extended mean survival in an orthotopic rat GBM RG2 model. Adapted with permission from song et al. [86], under the terms of a creative commons attribution license (https://creativecommons.Org/licenses/by/4.0/).

compared to saline-treated control animals (21.5 vs. 16 days), presumably due to limited tumor cellular uptake; conversely, EB-loaded PLA and PLA-HPG-CHO nanoparticles yielded the longest survival times (33 and 28 days), which may be attributed to their superior internalization efficiency within tumor cells.

Targeting GBM cells with specific moieties can also significantly enhance cell uptake. The local injection of DTX-loaded PLGA nanoparticles decorated with L-histidine (H, to target the tumor-overexpressed L-type amino acid transporter 1 [LAT1]), forming DTX-H-NPs in orthotopic U87MG GBM-bearing mice prompted significantly extended median survival times (46.5 days) compared to untreated mice (30 days) and those treated with DTX-loaded non-functionalized NPs (DTX-NPs; 33.5 days), and free DTX [99]. DTX-H-NP treatment also prompted a higher percentage of long-term survival over 60 days (37.5% vs. 0% for DTX-NPs) and 120 days (12.5% vs. 0% for DTX-NPs and free DTX, respectively). These results demonstrate that DTX-H-NP treatment significantly outperformed DTX-loaded non-functionalized-DTX-NPs, with the enhanced effect attributed to L-histidine's ability to improve GBM cell uptake and support higher DTX accumulation at the tumor site and a more potent therapeutic response.

Polymer-based nanoparticles have also been frequently applied during the development of gene delivery systems for localized administration in GBM; for instance, low molecular weight protamine (Pr; protein) and dextran sulfate (DEX; polysaccharide) formulations (Pr-DEX) have been investigated for

GBM treatment [100]. This study prepared Pr-DEX nanoparticles using a microfluidic-assisted ionic cross-linking method involving a model sequence of pDNA, micro(mi)RNA, or small-interfering (si)RNA assembled by charge-charge interaction. In vitro evaluations in 3D spheroids models of human GBM cell lines (U87MG, GIN-8, GIN-28, and GCE-28) and in vivo studies in zebrafish embryos demonstrated minimal toxicity, efficient internalization, and stable expression of fluorescent/luminescent proteins, which highlighted this formulation´s potential as an effective gene delivery system for GBM.

Polymer-based drug conjugates – as a sub-type of polymeric nanocarriers – also represent efficient DDSs; these pharmacologically active macromolecules comprise generally biodegradable polymers covalently conjugated to one or more therapeutic or diagnostic agents (e.g., small molecules, probe, peptides, proteins, or aptamers) via bioresponsive linkers. Conjugation offers several advantages over mere encapsulation, including improved drug solubility, controlled release, enhanced efficacy, and improved pharmacokinetics [101,102]. The use of polymer-drug conjugates has also extended to the localized treatment of GBM; for example, Zhang et al. prepared PEGylated and non-PEGylated poly(aspartic acid) (PAA)-cisplatin conjugates that supported controlled drug release at concentrations that eliminated tumor cells without causing the toxicity-related death observed following the CED of cisplatin into the brain [103]. The authors also employed PEGylation to enhance the penetration of conjugates throughout the brain parenchyma. The median survival time of rats with 9 L orthotopic gliosarcoma significantly improved following treatment with PEGylated PAA-cisplatin conjugates (median survival not reached; 80% long-term survivors) compared to non-PEGylated PAA-cisplatin conjugates (40 days), free cisplatin (12 days), or saline-treated controls (28 days).

In a related study, Artzi et al. elegantly engineered dual-sensitive nanoparticles (Dual-NPs) composed of a DEX nanoparticle surface-conjugated with polyamidoamine (PAMAM) dendrimers bearing doxorubicin (Dend-NPs) via dual-sensitive (matrix metalloproteinase [MMP]- and pH-cleavable) linkers [104]. This design allowed Dual-NPs to rapidly disassemble and gradually release Dend-NPs within the GBM TIME. The authors detected Dual-NPs at the tumor site for up to six days after a single intratumoral injection in an orthotopic mouse GL261-luc GBM model, which significantly delayed tumor growth and markedly improved survival (median survival: 30 days) compared to untreated mice (18 days) or those receiving free doxorubicin (DOX) and Dend-NPs (21 days and 22 days, respectively). Furthermore, Dual-NPs completely eliminated tumor cells in 25% of animals, with no evidence of residual tumor growth at two months post-treatment.

The advantages of treatment with polymer-based drug conjugates lie in their ability to carry multiple compounds with distinct mechanisms of action. For instance, our group developed an in situ chemoimmunotherapeutic approach comprising bio-responsive hyaluronic acid (HA)-drug conjugates, enabling the combination of therapeutic agents to enhance GBM treatment efficacy compared to free drugs [105,106]. We hypothesized that combining DOX, an immunogenic cell death inducer, with CpG oligodeoxynucleotides (a Toll-like receptor (TLR)-9 agonist that stimulates the immune system) would exert a synergistic anti-cancer effect when conjugated to HA (100 kDa). The HA-CpG conjugate reeducated alternatively activated M2-like microglia to a classically activated pro-inflammatory M1-like phenotype, while the HA-DOX conjugate boosted immunogenic cell death induction in GL261 GBM cells. In a GL261 GBM orthotopic mouse model, the simultaneous CED of the HA-DOX and HA-CpG conjugates triggered antitumor CD8+ T cell responses, reduced M2-like macrophage and myeloid-derived suppressor cell (MDSC) infiltration, and prompted long-term survival in over 66% of animals compared to the treatments. These results highlight the therapeutic potential of integrating synergistic agents within a single HA-based nanocarrier platform. Similarly, we also demonstrated that conjugating HA (100 kDa) to DOX (HA-DOX)and gemcitabine (GEM; HA-GEM) influenced localized tumor-associated myeloid cells, including macrophages and MDSCs [107]. Specifically, we observed that HA-DOX + HA-GEM treatment induced a reduction in M2-like macrophages and monocytic MDSCs and a shift toward a pro-inflammatory M1-like phenotype compared to untreated and free DOX + GEM treatment, contributing to improved tumor growth control and improved survival in two GBM orthotopic mice models (GL261 and SB28). As these strategies function by remodeling the GBM TIME toward a more inflamed, immunostimulatory state, we also explored the Stimulator of Interferon Genes (STING) pathway as a means to recruit innate and adaptive immune cells to the GBM TIME [108]. We conjugated HA to a non-nucleotide STING agonist (MSA2; HA-MSA2) for in situ GBM treatment; the localized delivery of HA-MSA2 in an orthotopic SB28 GBM mouse model delayed tumor growth and extended survival and markedly shifted in the immune landscape (compared to untreated and free MSA2-treated mice), which included the increased infiltration of dendritic cells, natural killer cells, and CD8+ T cells.

Finally, combining drug-loaded polymeric micelles with physical methods to transiently open the blood-brain barrier has been explored to improve therapeutic delivery to brain tumors. Lammers et al. screened different chemotherapeutic combinations in different GBM cell lines (including U87MG, GL261, KNS-42, and SF-8628) to identify a synergistic pairing of valrubicin (VAL) and panobinostat (PAN) aiming to next combine the most promising with FUS [109]. The authors encapsulated these two chemotherapeutics drugs within poly(ethylene glycol)-b-poly(N-2-benzoyloxypropyl methacrylamide) (mPEG-b-p(HPMA-Bz) polymeric micelles and intravenously injected them with FUS into a mouse GL261 GBM model. As the mice tolerated the double drug-loaded micelles well and demonstrated a significant reduction in tumor growth, they next evaluated this system in a more clinically relevant model – orthotopically implanted patient-derived HSJD-DIPG-007 diffuse intrinsic pontine gliomas characterized by an intact blood-brain barrier and resistance to conventional therapies – to further evaluate the platform´s efficacy with FUS. In this case, the intravenous delivery of double drug-loaded micelles combined with FUS-mediated blood-brain barrier disruption displayed enhanced therapeutic efficacy; in particular, these mice displayed a 2–3-fold reduction in tumor

burden by day 50 post-treatment compared to mice treated with the free forms of VAL + PAN.

4.1.3. Lipid nanoparticles

Lipid-based nanocarriers have emerged as promising platforms for localized drug delivery in GBM treatment. Among these, lipid nanocapsules (LNCs), lipid nanoparticles (LNPs), and liposomes have been extensively explored for their ability to enhance intratumoral drug retention, targeting, and therapeutic efficacy (Table 1). These approaches aim to overcome the limitations of systemically administered therapies by improving drug bioavailability and tumor specificity, with encouraging results in preclinical models.

Menei et al. designed sorafenib (SFN; a tyrosine kinase inhibitor)-loaded LNCs for CED in an orthotopic U87MG GBM mouse model [110]. While both SFN-loaded LNCs and free SFN reduced tumor growth compared to controls, SFN-loaded LNCs displayed a greater ability to promote early vascular normalization (as evidenced by increased perfusion and reduced tumor vessel area). GBM tends to possess a leaky vasculature and suffer from related blood flow impairments, and the potential perfusion increment provided by SFN-loaded LNCs might benefit combinational therapies involving, for example, TMZ. Moreover, treatment with SFN-loaded LNCs reduced the number of proliferative cells (Ki67+) in the tumor, an effect also observed after treatment with free SFN, probably due to the more rapid uptake of free SFN by tumor cells than endothelial cells; however, SFN-loaded LNCs did not significantly alter overall tumor growth despite these biological improvements, suggesting limited therapeutic impact.

In a similar study, Lollo et al. developed multifunctional LNCs to co-deliver PTX and CpG [111]. Coating LNCs with chitosan (CS) also facilitated CpG complexation and enabled robust interactions with GL261 GBM cells, consequently producing apoptotic effects; moreover, CED administration of PTX-CpG-LNCs in GL261 GBM-bearing mice resulted in prolonged survival (34 days) compared to saline-treated control mice (28 days) or those treated with free PTX (formulated as Taxol®, 28 days), the simple injection of PTX LNCs (31 days) or PTX LNCs + CpG (31 days).

Kadiyala et al. engineered synthetic high-density lipoprotein (sHDL)-mimicking nanodiscs composed of 1,2-dimyristoyl-sn-glycero-3-phosphocholine (DMPC) and 1-palmitoyl-2-oleoyl-glycero-3-phosphocholine (POPC) to locally deliver DTX and CpG (DTX-sHDL-CpG) into an orthotopic mouse GL261 GBM model, which prompted tumor regression and stimulated antitumor CD8+ T cell responses within the TIME without significant off-target side effects [112]. Simple RT lead to a survival of 43 days, while combining DTX-sHDL-CpG with RT resulted in tumor regression and long-term survival in 80% of GBM-bearing mice, which remained tumor-free after rechallenge with tumor cells in the contralateral hemisphere, indicating the development of anti-GBM immunological memory. A study by Halseth et al. obtained similar results when delivering GW396 (a Liver-X-Receptor agonist) and CpG within synthetic HDL-mimicking (CpG-sHDL) nanodiscs to target cholesterol metabolism and induce cancer cell death while promoting an immune response [113]. GW396-CpG-sHDL nanodiscs enhanced the expression of cholesterol efflux transporters in murine GL261 cells, which promoted the more significant removal of cholesterol. Importantly, GBM tumors display a reduced capacity to produce cholesterol and instead depend on the uptake of cholesterol produced by astrocytes [114]. The authors demonstrated in an orthotopic mouse GL261 model that combined GW396-CpG-sHDL + RT treatment significantly improved median survival compared to GW396-CpG-sHDL (median survival: 33 days) or RT alone (median survival: 34 days); additionally, 66% of long-term survivors in GW396-CpG-sHDL + RT-treated mice remained tumor-free when rechallenged with tumor cells.

Peer et al. functionalized LNPs containing siRNA targeting polo-like kinase 1 (*PLK1*; due to its role in driving cell cycle progression) with HA, which specifically binds the CD44 receptor expressed by GBM cells [115]. siRNA-containing HA-LNPs (HA-LNPs-siPLK1) effectively targeted GBM cell lines and primary neurospheres from GBM patients, while CED of HA-LNPs-siPLK1 significantly prolonged survival in an orthotopic mouse U87MG model and reduced target mRNA levels by more than 80% compared with control groups (saline-treated and HA-LNPs containing siRNA against luciferase; HA-LNPs-siLuc).

In another related study, Bi et al. employed polysarcosine (pSar)-based surface modification as an alternative to PEG to improve the stability and circulation of lipoplexes composed of 1,2-dioleoyl-3-trimethylammonium-propane (DOTAP) and dioleoylphosphatidylethanolamine (DOPE) when developing DDSs [116]. They synthesized four pSar-lipid conjugates with defined pSar average molecular weights (Mw – 2 and 5 kDa; 2K and 5K) and anchor diacyl chain lengths (14 and 18 carbon units; C14 and C18) and incorporated these lipids into cationic liposomes, which they complexed with green fluorescent protein (GFP) mRNA to form lipoplexes. While not yet evaluated in rodent GBM models, pSar-modified lipoplexes displayed enhanced transfection efficiency and biodistribution in zebrafish brains, particularly the C14-pSar2k formulation, providing proof-of-concept for potential applications in GBM.

Another notable strategy to overcome formulation limitations involved the encapsulation of topotecan into nanoliposomes using various components using a modified gradient-loading technique with a sterically hindered amine and highly charged anionic trapping agents (either polymeric (polyphosphate) or non-polymeric (sucrose octasulfate) [117–119]. This strategy enabled extremely high drug-to-lipid loading ratios (> 800 g drug-11/mol phospholipid), addressing a common bottleneck in nanoparticle-based chemotherapy (Table 1).

In the context of IAD, Joshi et al. investigated the impact of large (200 nm) and small (~60 nm) liposomes and the role of surface charge (cationic or neutral) on in vivo biodistribution [120]. The authors intra-arterially injected fluorescently labeled liposomes with different properties into C6 glioma-bearing Sprague Dawley rats after induction of IAD; overall, large cationic liposomes display the most significant accumulation in GBM tumors.

4.1.4. Inorganic nanoparticles

Inorganic nanoparticles represent a versatile class of nontoxic materials (including gold, silver, graphene-based, hydroxyapatite, iron, cerium, zinc oxide, and ceramics) that offer a broad range of physicochemical, mechanical, magnetic, and optical

properties [121]. Inorganic nanoparticle surfaces can be functionalized with targeting ligands to improve site-specific delivery, making them suitable for DDSs and advanced bio-imaging applications. The advantages of inorganic nanoparticles reside in their compatibility with multiple imaging modalities (e.g., luminescence, magnetic resonance, fluorescence imaging, and X-ray computed tomography) that allow extended imaging periods with improved signal-to-noise ratios [121].

In the context of GBM, several inorganic nanoparticle formulations have been developed to enhance therapeutic efficacy and diagnostic precision (Table 1); for instance, NanoTherm® - a ferrofluid formulation of amino silane-coated superparamagnetic iron oxide nanoparticles (SPIONs) of 15 nm in size used for localized thermal ablation – can be directly administered into GBM tumors and activated by an alternating magnetic field to generate localized hyperthermia to damage cancer cells while sparing healthy tissue [122]. Beyond direct cytotoxicity, the induced hyperthermia enhances tumor sensitivity to radiation and chemotherapy, potentially reducing recurrence rates.

Expanding on the theranostic capabilities of inorganic nanoparticles, Wu et al. designed a multifunctional nanoplatform employing hollow mesoporous organosilica nanoparticles (HMONs; synthesized employing SiO_2 as the hard template and bis(3-triethoxysilylproyl)disulfide (BTDS) with a disulfide bond group as the organosilica precursor) decorated with ultrasmall Cu_2−xSe particles and loaded with DOX [123] (Figure 4). This multifunctional theranostic nanosystem exhibited tumor-triggered programmed destruction facilitated by the reduction-responsive cleavage of disulfide bonds incorporated into the HMON framework. These bonds connect HMONs to the Cu_2−xSe particles (HMONs-ss-Cu_2-xSe; HCu), enabling tumor-specific biodegradation that occurs in response to elevated intracellular glutathione levels and supporting on-demand drug release following CED in orthotopic U87 glioma-bearing mice when coupled with FUS. DOX-HCu /FUS treatment induces the significant inhibition of tumor growth (91.1%) compared to the control group at day 22, displaying greater effectiveness than treatment with free DOX (35.4%), free DOX with FUS (69.2%), or DOX-HCu (52.4%). The study also noted a significantly longer median survival time in mice treated with DOX-HCu/FUS (52 days) than mice treated with FUS (24 days), free DOX (32 days), free DOX with FUS (42 days), and DOX-HCu (35 days). These findings underscore the importance of integrating responsive drug release mechanisms with targeted activation for precise glioma therapy.

Related studies have explored piezoelectric materials for sonodynamic therapy (SDT), a technique still undergoing optimization due to challenges related to blood-brain barrier penetration and unclear mechanisms of action. Wang et al. proposed that layered piezoelectric $SrBi_2Ta_2O_9$ (SBTO) nanoparticles covered with 1,2-distearoyl-sn-glycero-3-phosphoethanolamine-PEG2000-Transferrin (DSPE-PEG2000-Transferrin) to further overcome the BBB, could significantly depolarize the mitochondria and eliminate human GBM cells (U87MG) when exposed to FUS [124]; furthermore, the ultrasound-induced band bending in SBTO nanoparticles can enhance ROS generation. SBTO nanoparticles preferentially accumulated in mitochondria following FUS, disrupting the mitochondrial membrane potential and inducing apoptosis in U87MG-Luc cells. Moreover, SBTO nanoparticles crossed the blood-brain barrier after CED in orthotopic U87MG model mice and accumulated in GBM tumors through a combination of FUS-induced microbubbles and protein-mediated transport (SBTO nanoparticles + FUS). The study confirmed therapeutic efficacy via the significantly improved survival in combination with FUS (35 days, + 67%) compared to control.

Overall, polymer-based, lipid-based, and inorganic nanoparticles offer distinct advantages for localized GBM treatment, ranging from controlled drug release and efficient cellular uptake to imaging and stimulus-responsive therapies; overall, they provide a complementary toolkit for enhancing efficacy in localized GBM therapy.

4.2. Drug delivery systems for post-operative glioblastoma

4.2.1. Key approaches for designing drug delivery systems for resected glioblastoma

The surgical resection cavity left after GBM tumor removal presents a distinct local environment for therapeutic intervention, characterized by irregular geometry, dynamic fluid exchange, and the presence of residual tumor cells at the margins [125]. The localized application of DDSs into the post-operative GBM resection cavity represents an appealing approach for the prolonged and sustained release of GBM therapeutics and the resected TIME [80,126]; nevertheless, effective DDSs must satisfy multiple critical design criteria. Securing appropriate drug release kinetics alone or when combined with other drugs to guarantee successful tumor treatment remains the primary goal; ideally, applied DDSs should demonstrate an initial burst release followed by zero-order controlled release, maintaining a constant drug concentration within the therapeutic window at the tumor site over an extended period [127,128]. Factors influencing drug release kinetics include loading, solubility, diffusion coefficients, and matrix degradation rates for biodegradable DDS. In addition, DDS should display biocompatibility and cause no harm to healthy brain tissue [127,128]; this includes the possession of suitable mechanical properties that match brain tissue stiffness, thereby preventing a foreign body response [128] (Figure 5).

4.2.2. Hydrogels

Hydrogels have emerged as promising platforms for localized drug delivery in GBM therapy, especially in the context of post-surgical treatment (Table 2). The ability of hydrogels to form implantable depots at the tumor resection site allows for the sustained and localized release of therapeutics, minimizing toxicity and recurrences while improving drug retention and efficacy [129]. Integrating nanoparticles into these hydrogels supports the fine-tuning of drug release kinetics and the incorporation of multiple functions such as targeting, responsiveness to tumor-specific enzymes, and combination therapies [41,130].

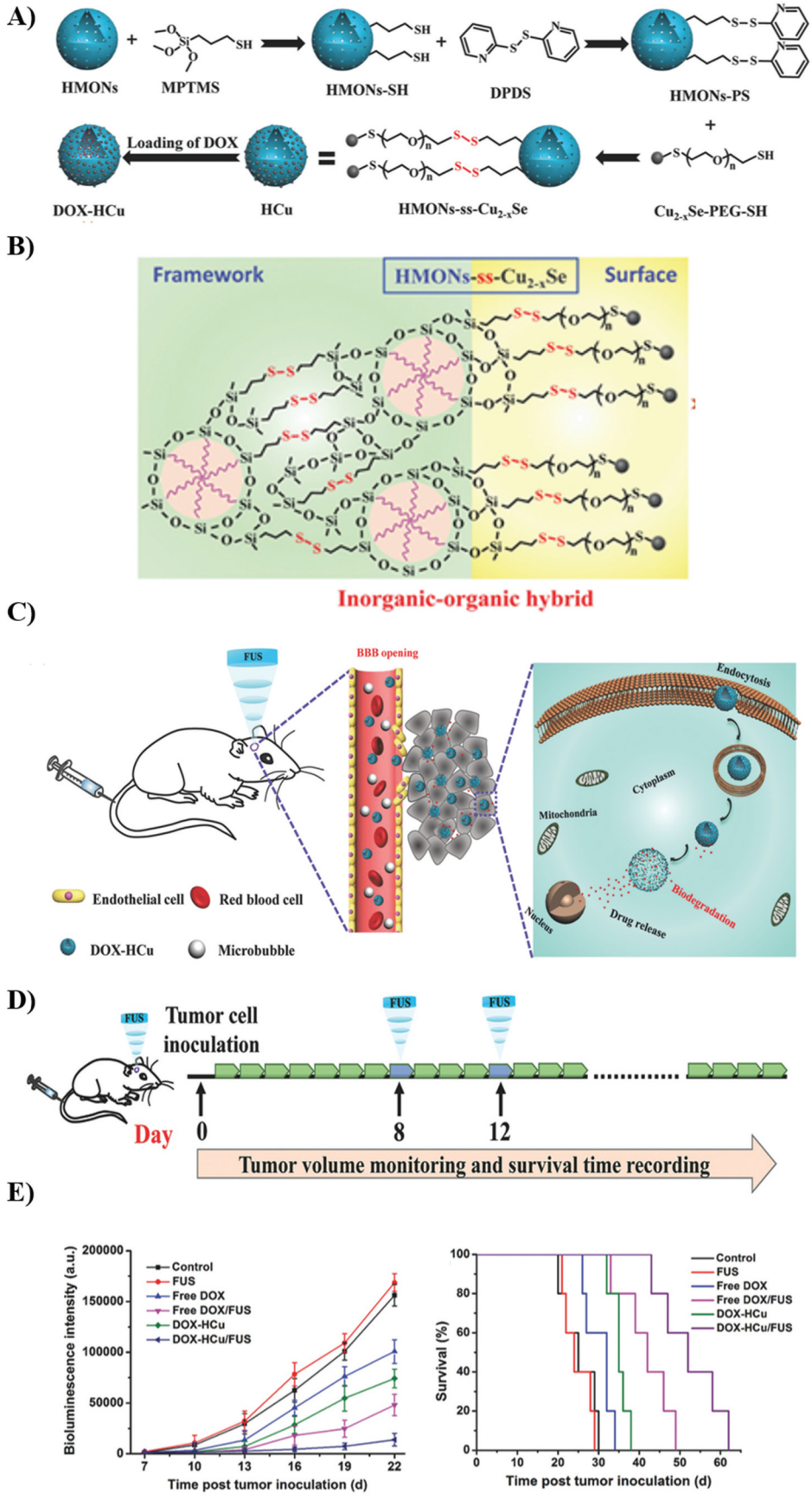

Figure 4. A biodegradable theranostic nanoplatform: focused ultrasound-mediated delivery of hollow mesoporous organosilica nanoparticles to an orthotopic mouse U87MG glioblastoma model. (A) Schematic representation of the synthesis of hollow mesoporous organosilica nanoparticles (HMONs) connected to Cu_2−xSe particles via disulfide binds (HMONs-ss-Cu_2-xSe; HCu). Abbreviations: 3-mercaptopropyltrimeth oxysilane (MPTMS), HMONs modified with sulfhydryl groups via MPTMS grafting (HMONs-SH), 2,2′-dipyridyl disulfide (DPDS), HMONs-SH modified with DPDS (HMONs-PS), ultrasmall Cu_2−xSe particles (Cu2-xSe-PEG-SH) (B)

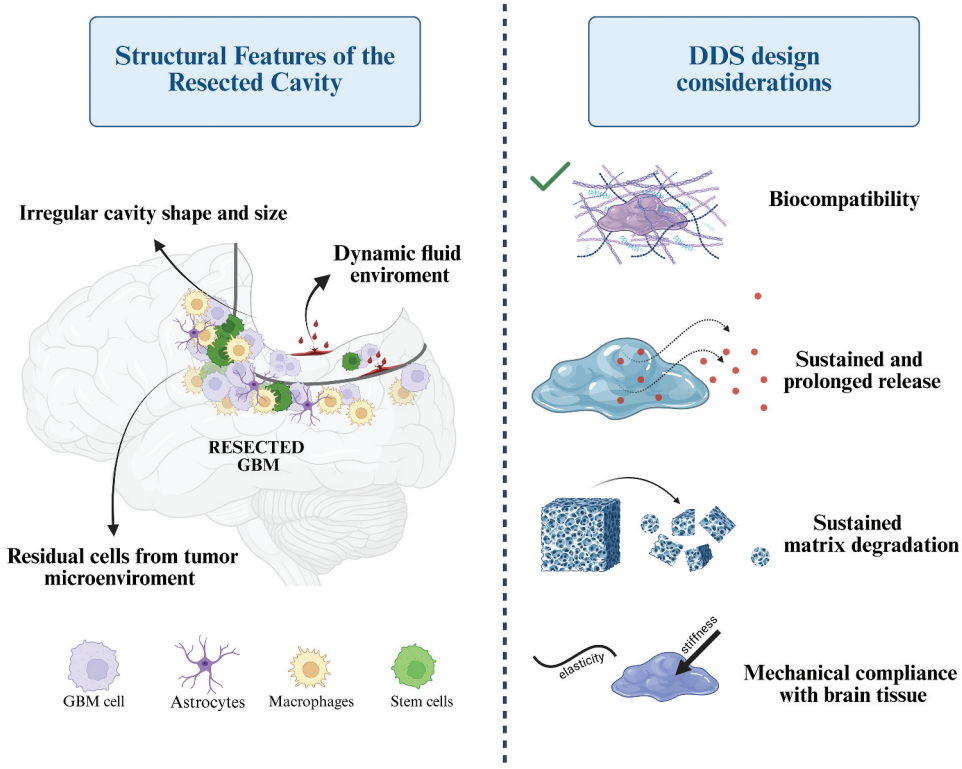

Figure 5. Challenges and design considerations for local drug delivery for resected GBM. The design of drug delivery systems for resected tumors should meet several requirements. DDS has to adapt to the irregularities of the brain cavity; moreover, the selection of the therapeutics should be done considering the resected TIME that involves different subsets of cells (e.g., astrocytes, stem cells, cancer cells, etc). While achieving appropriate drug release kinetics (preferentially zero-order-controlled release) represents the primary goal, other factors that enter into consideration include drug diffusion coefficient, solubility, and loading; furthermore, the selected matrix of the drug delivery system should be biodegradable, and mechanical properties must match brain stiffness. Created in https://BioRender.com.

Researchers from the Préat laboratory have worked extensively in the development of LNC-based hydrogels loaded with drugs such as GEM [131], DOX [132], PTX [133], and salinomycin [134] (and their derivatives) to achieve tailored drug release in the resection cavity in different GBM models (U87MG, 9 L, and GL261); overall, their work has demonstrated promising preclinical outcomes.

In a related study, Bastiat et al. functionalized GEM-loaded LNCs (GEM-LNCs) with the neurofilament light subunit-tubulin -binding-site 40–63 (NFL-TBS) peptide (GEM-NFL-LNCs), which binds the tubulin subunits overexpressed by GBM cells [135]. The authors decorated LNCs by peptide adsorption onto the nanocarrier's surface. In vivo studies in an orthotopic mouse U87MG GBM resection model provided evidence that a GEM-NFL-LNC hydrogel targeted non-resected GBM cells and significantly delayed or inhibited disease recurrence; overall, GEM-NFL-LNC hydrogel treatment significantly extended median survival (74 days), outperforming both untreated (38 days) and a non-targeted GEM-LNC hydrogel (44 days).

Zhao et al. developed an injectable MMP-responsive triglycerol monostearate (Tm) hydrogel loaded with TMZ and O6-benzylamine (BG; an MGMT inhibitor) to eradicate residual post-operative TMZ-resistant GBM cells [136]. The authors engineered the Tm hydrogel to release drugs in response to the high concentrations of MMP enzymes observed after GBM surgery. The localized application of the TMZ-/BG-laden Tm hydrogel into the resected cavity following the removal of an orthotopic rat C6 TMZ-resistant GBM cell-derived tumor in a nude mouse model demonstrated the synergistic activity of the two drugs compared to locally administered free TMZ inducing an extension of the survival (54.5 vs 39.5 days).

The application of PDT by placing free or DDS-formulated photosensitizing agents within a hydrogel situated in the resected GBM cavity represents an interesting treatment option. For example, Cao et al. developed a DDS for the localized treatment of postoperative GBM [137], which comprised a photosensitizer – Chlorin e6 (Ce6) – conjugated to chemiluminescent luminol-loaded PTX prodrug nanoparticles and copper peroxide nanodots co-embedded within a 3D thermosensitive hydroxypropyl chitin hydrogel framework (CP-CL-NP_{PTX}-Gel). After injection into the cavity of the post-operative orthograph mouse U87MG model, CP-CL-NP_{PTX}-Gel cross-links into a gel at body temperature to serve as a drug reservoir that considerably prolongs the retention time of the

Schematic representation of the composition and biodegradable behavior of HCu nanoparticles loaded with doxorubicin (DOX-HCu). (C) Graphic representation of enhanced delivery of DOX-HCu into the brain tumor following focused ultrasound (FUS)-induced blood-brain barrier (BBB) opening and DOX-HCu degradation caused by elevated levels of glutathione (GSH) in the tumor microenvironment. (D) in vivo therapeutic scheme of FUS-mediated chemotherapy in an orthotopic mouse U87MG glioblastoma model. (E) bioluminescence signal over time and survival curves of model mice receiving various Treatments. Adapted from Wu et al. With permission [123], under the terms of a creative commons attribution license (https://creativecommons.Org/licenses/by/4.0/).

Table 2. Relevant examples of preclinical hydrogels, implants, and scaffolds for post-operative glioblastoma treatment.

Materials used for implants and scaffolds	Delivery route	Drug	Device	Dose	GBM model	Outcome	References
Hydrogels							
LNCs made of Labrafac® Span 80 Kolliphor® HS15	In situ implantation	GEM	LNC Hydrogel	3 mg/kg	Orthotopic mouse U87MG model	**Survival**: Untreated: 35.5 days Empty LNC Hydrogel: 38 days Free GEM: 61 days GEM-LNC hydrogel: 62 days	[131]
LNCs made of Labrafac® Span 80 Kolliphor® HS15 Cytidine-C_{16}	In situ implantation	DOX	LNC Hydrogel	5 mg/kg	Orthotopic mouse GL261 model	**Survival**: Untreated: 29 days Empty LNC Hydrogel: 29 days DOX-LNC Hydrogel: 37 days	[132]
LNCs made of Span80 Kolliphor® HS15 Labrafac® Schol Didodecyldimethylammonium bromide Sodium cholesteryl sulfate	In situ implantation	$GEMC_{12}$ + NFL	LNC Hydrogel	$GEMC_{12}$ (2 mg/kg), NFL (4.5 mg/kg)	Orthotopic mouse U87MG model	**Survival**: Untreated: 38 days $GEMC_{12}$-LNC Hydrogel: 44 days $GEMC_{12}$-NFL-LNC Hydrogel: 74 days	[135]
Tm	In situ implantation	TMZ + BG	MMP-responsive Hydrogel	–	Orthotopic rat C6 TMZ-resistant GBM cell-derived tumor in nude mice	**Survival**: Untreated: 25.5 days Empty-Tm hydrogel: 33.5 days Intravenous TMZ: 36.5 days TMZ-Tm Hydrogel: 39.5 days TMZ+BG-Tm hydrogel: 54.5 days	[136]
CP CL c(RGDyD) peptide	In situ implantation + PDT	PTX + CP + Ce6	Thermosensitive Hydrogel	–	Orthotopic mouse U87MG model	**Tumor Growth**: CP-CL-NP_{PTX}-Gel prolonged drug retention time in the postoperative cavity and increased survival time of postoperative glioma mice	[137]
PEG750-pCL-co-TMC PEG DMA	In situ implantation	TMZ	Photopolymerizable Hydrogel	4.75 mg/kg	U87MG Mouse Orthotopic	**Tumor Growth**: M-TMZ-PEG-DMA Hydrogel significantly reduced tumor weight, with tumors completely disappearing in two animals	[138]
BSA CMC-g-PNIPAAmMA $DTPA_{Gd}$/bPEI	In situ implantation + MRI	EPI + PTX	Theranostic Hydrogels	EPI (1 mg) PTX (0.1 mg)	U87MG and MBR614 mouse gliosarcoma model	**Survival**: **U87MG** Control: 27 days BSA nanoparticle hydrogel: 27 days EPI hydrogel: 48 days BSA-PTX hydrogel: 34 days BSA-PTX-EPI hydrogel: 69 days; median survival not reached. **MBR614** Control: 18 days EPI hydrogel: 32 days BSA nanoparticle hydrogel: 21 days BSA-PTX-EPI hydrogel: 63 days; median survival not reached	[139]

(*Continued*)

Table 2. (Continued).

Materials used for implants and scaffolds	Delivery route	Drug	Device	Dose	GBM model	Outcome	References
MPDA M1NVs Fibrinogen THR	In situ implantation + PDT	DOX	Fibrin Hydrogel	–	Orthotopic mouse GL261 model	**Survival**: Hydrogel: 20 days MPDA-M1NVs Hydrogel: 32 days MPDA Hydrogel+PDT: 30 days MPDA-DOX Hydrogel+PDT: 62 days MPDA-DOX-M1NV Hydrogel: 63 days; median survival not reached	[140]
Lipoic acid Fe^3	In situ implantation	αPD-L1	Lipoic acid Fe^{3+}-based hydrogel	–	Orthotopic mouse GL261 model	**Survival**: Control: Not reported LFH hydrogel: 27 days LFH-αPDL1 hydrogel: 38 days	[141]
iRGD PTX	In situ implantation	PTX + αCD47	Self-assembling PTX-RGD filament hydrogel	PTX (150 μg), αCD47 (50 μg)	Orthotopic mouse GL261 model	**Survival**: Untreated: 28.5 days PTX Hydrogel: 29.5 days αCD47+PTX Hydrogel: 39 days αCD47-PTX-RGD Hydrogel: 80 days; median survival not reached	[142]
Scaffolds and Implants							
Ace-DEX PLA	In situ implantation	DOX	Ace-DEX/PLA scaffolds	200 μg	Orthotopic mouse U87MG model	**Survival**: Ace-DEX-DOX: 100% survival PLA-DOX: 63 days	[145]
Ace-DEX	In situ implantation	PTX	Ace-DEX scaffold	75 μg	Orthotopic mouse U87MG resection model	**Survival** (OS%) Ace-DEX (fast release)-PTX + Ace-DEX (slow release)-PTX: 78% Ace-DEX (fast release)-PTX: 44% Ace-DEX (slow release)-PTX: 50% Ace-DEX (mid-release)-PTX 20%	[146]
Ace-DEX	In-situ implantation	PTX + EVR	Ace-DEX scaffold	U87MG PTX (75 μg) EVR (20 μg) LN-229 PTX (50 μg) EVR (20 μg)	U87MG and LN-229 Mouse Orthotopic	**Survival (OS%) in U87MG** Ace-DEX-PTX: 50% Ace-DEX-EVR: 0% Ace-DEX-PTX-EVR: 100% **Survival (OS%) in LN-229** Ace-DEX-PTX: 20% Ace-DEX-EVR: 0% Ace-DEX-PTX-EVR: 100%	[147]
PLGA-PEG	In situ implantation	OLA + TMZ+ ETOP	Paste	Incremental doses of drugs alone/in combination in %w/w	F344 immunocompetent rat 9 L model	**Survival (OS%)**: 10% OLA paste: 28% 20% OLA paste: 28% 10% OLA + 20% TMZ paste: 57% 20% OLA + 20% TMZ paste: 43% 10% OLA + 20% ETOP paste: 57% 20% OLA + 50% ETOP paste: 71%	[148]
PLGA Poloxamer-188	In situ implantation	IRT	iDES	Incremental dose of IRT	Orthotopic mouse U87 mCherry-Fluc GBM model	**Survival**: iDES IRT 30% w/w: 40% iDES IRT 40% w/w: 40%	[151]
PLA PLGA Magnesium-based electronic device Oxidized starch	In situ implantation	DOX + Temperature	BEP	DOX (0.69 mg)/heating	Orthotopic mouse U87MG and canine J3T–1 models	**Survival**: DOX: 0% Empty BEP + heating: 0% BEP: 67% Gliadel wafer-like: 0% BEP + heating: 86%	[152]

(*Continued*)

Table 2. (Continued).

Materials used for implants and scaffolds	Delivery route	Drug	Device	Dose	GBM model	Outcome	References
PLGA PVA	In situ implantation	DTX + DICL	µMESH + Polymer-based nanoparticles	Intravenous TMZ (3 mg/kg every other day) Intravenous DTX (3 mg/kg every other day) For DTX + DICL and DTXL + DICL-µMESH (both DTXL and DICL 0.75 mg/kg)	U87MG and hCSCs GBM Mouse Orthotopic	**Survival in the U87MG model**: µMESH-DTX + DICL: 90% **Survival in the hCSC model**: µMESH-DTX + DICL: 100%	[153]
PLGA PVA	In situ implantation	DTX + PTX	µMESH + Polymer-based nanoparticles	DTX (0.75 mg/kg) PTX (0.75 mg/kg)	Orthotopic Mouse U87MG model	**Survival**: Control: 32.5 days NanoPTX-µMESH: 75 days PTX-µMESH: 90 days NanoDTX-µMESH: N/A – 60% of animals survived 90 days DTX-µMESH: N/A – 80% of animals survived 90 days	[154]
Silk	In situ implantation	TMZ + BEV + THR	Silk fibroin microneedle patch	THR (0.3 U) TMZ (0.2 mg) BEV (30 mg) TMZ i.v. (50 mg/kg per day) BEV i.v. (10 mg/kg)	Orthotopic Mouse U87MG and U251MG models	**U87MG model** Control: 26 days Intravenous TMZ+BEV: 33 days THR+TMZ+BEV/Silk Patch: 41 days **U251MG model** Control: 30 days Intravenous TMZ+BEV: 39 days THR+TMZ+BEV/Silk Patch: 55 days	[156]

Abbreviations (alphabetical order): Ace-DEX: acetalated dextran; αPD-L1: anti-Programmed death-ligand 1; BEV: Bevacizumab, BEP: Biodegradable electronic device; BG: O6-benzylguanine; BSA: Bovine Serum Albumin; Ce6: chlorin e6; CL: Ce6-luminol-PEG(2000)-DSPE; CMC-g-PNIPAAmMA: Carboxymethyl cellulose-grafted poly(N-isopropylacrylamide- co-methacrylic acid); CP: Copper peroxide; DICL: Diclofenac; DOX: doxorubicin; DTPAGd/bPEI: Gadopentetic acid/branched polyethyleneimine; DTX: Docetaxel; EPI: Epirubicin; ETOP: etoposide; EVR: Everolimus; GEM: Gemcitabine; iDES: IRT-loaded Drug Eluting Seeds; IRT: Irinotecan; LFH: Lipoic acid Fe^{3+}-based hydrogel; LNC: Lipid nanocapsule; MMPs: Matrix metalloproteinase; MRI: Magnetic resonance imaging; MPDA: mesoporous polydopamine; M-TMZ: TMZ-loaded micelles; M1NVs: M1 macrophage-derived nanovesicles; NFL: NFL-TBS.40–63 peptide; OLA: Olaparib; PDT: photodynamic therapy; PEG: polyethylene glycol; PEG DMA: poly(ethylene glycol) dimethacrylate; PEG750-pCL-co-TMC: PEG750-Poly(ε-caprolactone-co trimethylene carbonate); PLA: Polylactic acid; PLGA: poly(lactide-co-glycolide); PTX: Paclitaxel; PVA: polyvinyl alcohol; THR: thrombin; Tm: Triglycerol monostearate; TMZ: Temozolomide; XRT: X-ray Therapy; µMESH: Hierarchically engineered polymeric implant.

drug in the postoperative cavity and extends the postoperative survival time compared to controls (Table 2).

Photopolymerization methods have also been employed to create hydrogel-nanostructure composites for GBM treatment. Danhier et al. designed TMZ-loaded PEG and poly(ε-caprolactone-co-trimethylene carbonate) (PEG750-pCL-co-TMC) micelles (M-TMZ) that they then loaded into a hydrogel composed of a PEG dimethacrylate (PEG DMA) network cross-linked with an ultraviolet source using a Lucirin-TPO (2,4,6-trimethylbenzoyldiphenyl phosphine oxide) photoinitiator [138]. This approach allowed precise control over hydrogel formation and the creation of a localized drug depot after in situ implantation; overall, the M-TMZ PEG-DMA hydrogel significantly reduced tumor growth and increased apoptosis compared to systemic TMZ treatment. Furthermore, tumors completely disappeared in two animals. The authors suggested potential compatibility with PDT, hinting at a modular strategy for combining phototherapy and localized chemotherapy.

Theranostic hydrogels represent an innovative evolution of localized GBM treatment, offering multifunctionality beyond simple drug delivery. These dual systems enable sustained therapeutic action at the resection site and real-time treatment monitoring. As an example, Lin et al. developed a theranostic hydrogel formulation with rapid gelation composed of carboxymethyl cellulose-grafted poly(N-isopropylacrylamide-co-methacrylic acid) (CMC-g-PNIPAAmMA), gadolinium (MRI agent), epirubicin (EPI), and PTX-loaded albumin nanoparticles [139]. Gliosarcoma model mice (MBR-614) or GBM (U87MG cells) treated with BSA-PTX-EPI hydrogel displayed increased survival (from 18 to 63 days for MBR-614; 27 to 69 days for U87MG) compared to controls (untreated and free drugs). MRI confirmed localized retention and gradual degradation of these theranostic hydrogels over 21 days, validating their role in treatment and imaging.

Chemo-immunotherapy – an innovative cancer treatment – stimulates the immune system to target and destroy tumors while minimizing damage to healthy tissues. Zhang et al. developed an injectable nanoparticle–hydrogel system that uses DOX-loaded mesoporous polydopamine (MPDA) nanoparticles encapsulated within M1-like macrophage-derived nanovesicles (M1NVs) supported by a fibrin gel matrix [140]. This chemo-immunotherapeutic platform (MPDA-DOX-M1NV hydrogel) triggered robust immune reprogramming at the tumor site when in situ implanted and activated by near-infrared light (PDT) in an orthotopic mouse GL261 model, where it converted immune-suppressive M2-like tumor-associated macrophages into a pro-inflammatory M1-like state, induced intense T cell infiltration and T cell effector function restoration, and reduced the number of suppressive immune cells (MDSCs and Tregs), ultimately enhancing tumor clearance and immune memory.

In another immune-engineering approach, Jia et al. developed an injectable lipoic acid-Fe^{3+} hydrogel (LFH) that could adapt to the mechanical properties of various brain tissues (including those of humans) through the coordination of Fe^{3+} ions within a hybrid network of lipoic acid [141]. When injected into the brain resection cavity, LFH undergoes spontaneous degradation in interstitial fluid, releasing lipoic acid and Fe^{3+} ions, which promote continuous ROS generation, ferroptosis, and immunogenic cell death in an orthotopic mouse GL261 model. When the team loaded LFH with an αPD-L1 (Programmed death-ligand 1) antibody, the resultant LFH-αPDL1 hydrogel amplified anti-tumor immune responses and enhanced ferroptosis locally, promoting superior CD3+CD8+ cytotoxic T cells without toxicity. Interestingly, the LFH form engineered to match the stiffness of mouse brain tissue (337 ± 8.06 Pa) effectively maintained normal brain water content (77%) and did not trigger astrocyte activation or hypertrophy, thereby preventing brain edema and scar formation.

Finally, Wang et al. designed a self-assembling PTX hydrogel comprising PTX and an iRGD peptide (PTX-RGD) that enhanced macrophage-mediated immune responses when in situ implanted for the localized treatment of recurrent GBM [142]. Aqueous PTX-iRGD solutions can form solid fibrils that can be directly applied to tumor resection cavities; additionally, embedding the immune checkpoint inhibitor αCD47 with the hydrogel provided cavity filling and long-term release of PTX and αCD47, which play a crucial role in regulating a macrophage-mediated phagocytosis. PTX creates a pro-inflammatory TIME, facilitating macrophage phagocytosis and stimulating a robust T-cell response. In an orthotopic mouse GL261 model, the αCD47-PTX-RGD hydrogel significantly delayed tumor recurrence and improved survival (39 days) with minimal systemic toxicity compared to mice treated with PTX hydrogels (29.5 days).

4.2.3. Scaffolds and implants

To improve localized drug delivery post-resection in GBM patients, scaffolds and implants must integrate within brain tissue to ensure stable positioning, minimize off-target diffusion, and maintain compatibility with the brain's mechanical environment [143]. Given the highly mechanosensitive nature of brain cells, DDSs must exhibit viscoelastic properties similar to brain parenchyma to prevent inflammatory responses, gliosis, and increased intracranial pressure [41]. Flexible and conformable materials such as fibers, molds, and polymeric pastes have emerged as ideal candidates; their ability to adapt to the complex geometry of the resection cavity maximizes surface contact with the surrounding tissue, improving drug distribution and retention.

Acetalated dextran (Ace-DEX) nanofibrous scaffolds have been designed for various therapeutic applications, including the localized delivery of therapeutics into the resected GBM cavity [144]. Examples of Ace-DEX scaffolds (prepared via electrospinning) display various degradation rates (fast, medium, and slow) to support a wide range of drug release kinetic profiles. Several studies have reported the entrapment of various chemotherapeutics – including DOX [145], PTX [146], and everolimus in combination with PTX [147] – within Ace-DEX scaffolds. For example, PTX-loaded Ace-DEX scaffolds released 14.1%, 2.9%, and 1.3% PTX per day, respectively, according to the matrix's density and degradation rate. In a mouse U87MG GBM resection mouse model, the combination of a fast- and a slow-release scaffold (Ace-DEX (fast release)-PTX + Ace-DEX (slow release)-PTX) resulted

in 78% long-term survival, compared to only 20% survival in Ace-DEX (mid-release)-PTX group [146]. On the other hand, PTX released from Ace-DEX at fast and slow rate induced a median survival of 44 and 50%, respectively. This demonstrates the advantage of tailoring release profiles to target residual cells and long-term recurrence. The encapsulation of PTX and everolimus (EVR) into Ace-DEX (Ace-DEX-PTX-EVR) provided 100% survival in orthotopic mouse U87MG and LL-229 models compared to free drugs [147] (Table 2).

Rahman et al. developed biodegradable PLGA-PEG microparticles loaded with olaparib (OLA; a poly adenosine diphosphate-ribose polymerase-1 [PARP1] inhibitor) and etoposide (ETOP; a topoisomerase II inhibitor) [148,149]. The application of the PLGA-PEG delivery system as a paste during surgery in the GBM resection cavity supported the synergism of OLA + ETOP with oral TMZ (further potentiation possible with RT), which induced long-term survival in F344 immunocompetent rats bearing 9 L high-grade GBM tumors. Results showed that the combination of 20% olaparib + 50% etoposide (20% OLA + 50% ETOP paste) embedded into the paste led to 71% overall survival of rats treated compared to the remaining groups (See Table 2).

Grayson et al. designed polymeric microchips with membrane-covered reservoirs shaped as flat discs made from PLA and PLGA that passively released therapeutics from the reservoir at a rate dependent on membrane composition [150]. A study of microchips designed to deliver carmustine to a 9 L rat gliosarcoma model revealed 50% drug release within 12 h, followed by 20% over the next 6.5 days. Although the authors did not directly measure survival, carmustine-loaded microchips significantly reduced median tumor volume compared to controls (1.5 cm^3 vs. 15.0 cm^3).

Gawley et al. developed IRT-loaded drug-eluting seeds (iDES) composed of PLGA and Poloxamer-188 for in situ implantation into the margin of the GBM resection cavity to deliver sustained highly localized IRT doses while minimizing systemic toxicities [151]. iDES production employed a hot melt extrusion process, ensuring accurate IRT loading and maintaining the same cytotoxicity as free IRT. iDES released IRT in a sustained manner over 7 days; however, only the 30%, 40%, and 50% w/w-loaded iDES formulations released the 300–1000 µg of drug required for in vivo effectiveness. The 30% and 40% w/w-loaded iDES formulations significantly extended survival from 27 to 70 days in a U87 mCherry-Fluc GBM xenograft mouse resection model, with no signs of tumor recurrence. Additionally, the 30% w/w-loaded iDES formulation induced similar toxicity to placebo in non-tumor-bearing mice. These findings underscore the importance of achieving the correct dose-release balance and validate the feasibility of iDES as a simple yet effective postoperative implant.

Biodegradable DOX-loaded patches of oxidized starch have been integrated with magnesium-based wireless electronics to allow controlled intracranial drug release by remotely heating the system to brain tumors after localized application [152] (Figure 6). This bioresorbable electronic patch (BEP) ensured complete contact with the GBM resection cavity and featured a dual-surface design to prevent drug leakage into the cerebrospinal fluid. The biodegradation of the BEP helps minimize potential neurological side effects. In mouse (U87MG) and canine (J3T–1) GBM models, BEPs induced superior tumor suppression and survival compared to Gliadel wafers, highlighting their potential for clinical translation and individualized control.

A conformable polymeric implant (µMESH) for the continuous and direct delivery of drugs into the adjacent tumor bed has also been developed [153,154]. µMESH synthesis involved intercalating PLGA edges over arrays of polyvinyl alcohol (PVA) pillars for the sustained delivery of chemotherapeutic drugs such as DTX and PTX. The authors engineered four different µMESH configurations, encapsulating DTX or PTX within the PLGA micro-network (µMESH configurations) and encapsulating the two drugs within the PVA microlayer (nano-µMESH configurations). All µMESH configurations provided sustained drug release for months, with a simultaneous burst release observed within the first four days. In vivo, the peritumoral deposition of µMESH 15 days after GBM cell grafting in nude mice improved overall animal survival, which increased from ~30 days for untreated controls to 75 and 90 days for nanoPTX-µMESH and PTX-µMESH. Experiments employing DTX did not reach median survival, as 80% and 60% of animals treated with DTX-µMESH and nanoDTX-µMESH remained alive at 90 days. Exposure of a murine U87MG orthotopic GBM and of hCSC models to µMESH formulations containing DTX and diclofenac (DICL; 0.75 mg kg^{-1} of both drugs) abrogated disease recurrence for up to 8 months after tumor resection with no appreciable adverse effects. Without tumor resection, µMESH increased median overall survival rates (~30 days) as compared to the one-time intracranial deposition of DTX-loaded µMESH (15 days) or 10 cycles of systemically administered TMZ (12 days).

Silk microneedle patches – biodegradable implants made of silk fibroin – can deliver multiple therapeutic compounds at independent dosing amounts [155]. The bioresorbable device comprises silk protein mixed with therapeutic agents injected into a mold with needlelike projections, allowing different compounds to be loaded in specific device regions. Wang et al. delivered bevacizumab (BEV), TMZ, and thrombin (THR) using a silk microneedle patch into the resection cavity of U87MG resected GBM mice. Results showed that silk microneedle loaded with BEV+TMZ+THR showed a median survival of 41 days compared to intravenous administration of BEV +TMZ (33 days) and controls (26 days) [156]. Similarly the same formulations has been administered in U251MG human GBM model) [156]. Mice treated with THR+TMZ+BEV in the silk patch displayed a significantly longer median overall survival rate (55 days) compared to those treated with intravenous TMZ+BEV (39 days).

These studies converge on a common paradigm shift in GBM treatment: replacing systemic, high-toxicity chemotherapy with implantable, precision drug delivery platforms that offer controlled, localized, and long-term efficacy.

4.3. Localized treatment of glioblastoma with drug delivery systems: overview of clinical trials

The impact of the therapeutic approaches discussed above highlights advantages/disadvantages regarding efficiency

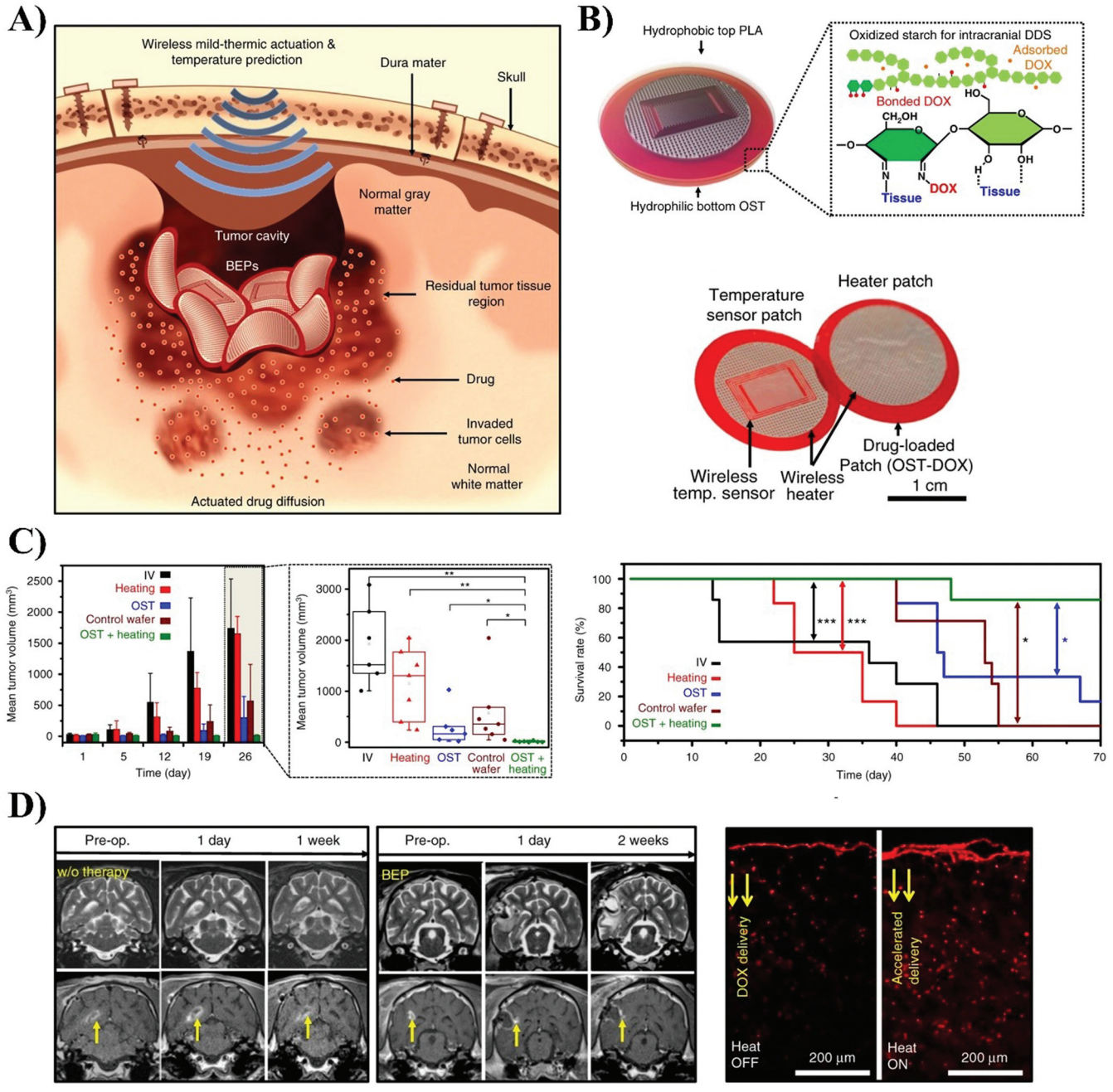

Figure 6. Bioresorbable electronic patch for drug delivery to brain tumors. (A) Schematic representation of the bioresorbable electronic patch (BEP) mechanism of action. (B) Image of a BEP, including a wireless heater and a temperature sensor on an oxidized starch patch (OST) containing doxorubicin (OST-DOX). (C) Therapeutic efficacy of the OST in a BALB/c nude mouse model of GBM regarding mean tumor volume, tumor volume at day 26 after surgery, and survival curves, showing significant improvements when applying OST and heating. (D) *left*: MRI images of the tumor without and with OST treatment in a J3T–1 canine brain tumor model. *Right*: fluorescence images of DOX diffusion from the OST into the tissue of the canine model without and with mild-thermic actuation. Adapted from [152], under the terms of a creative commons attribution license (https://creativecommons.Org/licenses/by/4.0/).

and safety. Each DDS strategy has shown some success in treating GBM in preclinical studies, and trials assessing their use with concurrent pharmacological intervention have shown significantly increased concentrations of the utilized agent within the desired target. Since the approval of Gliadel, there has been an increased interest in developing DDS for the local administration of therapeutic agents as a long-term strategy to treat GBM. Although numerous DDS have shown promising results in preclinical studies in these 25 years, their clinical translation remains limited. Although only a handful of studies have reported on human disease outcomes, early-phase clinical evaluations reveal promising but modest improvements in overall survival, underscoring the clinical potential and the need for further combination of DDS and clinical practice. Several recent reviews have comprehensively summarized the various DDS approaches and their primary outcomes [41]. This section will briefly focus on the few DDSs that have progressed to clinical trials in recent years (Table 3). Notably, compared to the trials performed at the beginning of the 1990s till the early 2000s, current trials have included

Table 3. Examples of recent clinical trials utilizing nanocarriers for the localized treatment of glioblastoma.

Trial number	Phase	Delivery Route	Formulation	Drug and Dose	Recruitment Status	Outcome	Reference
NCT02022644	I	CED	Nanoliposomal	Irinotecan (20–640 mg/mL, infusion volume 2–17 mL)	Active, not recruiting	Study results not submitted	[157]
NCT03566199	I/II	CED	Gold nanoparticle (MTX110)	Panobinostat (total volume 3–12 mL)	Completed	Overall survival of 26.1 months	[158]
NCT01906385	I/II	CED	NanoLiposome	Rhenium-186 (starting absorbed dose is 1 mCi in a volume of 0.660 mL)	Recruiting	Study results not submitted	[159]
NCT06271421	Not applicable	Implant	SPIONS for cyclic Hyperthermia (NanoPaste)	112 or 335 mg/ml of SPIONs	Recruiting	Study results not submitted	[160]
NCT04135807	Early Phase I	Implant	Implantable microdevice reservoirs releasing drugs – in situ implantation	Temozolomide Lomustine Irinotecan Carboplatin Lapatinib Osimertinib	Recruiting	Study results not submitted	[161]

Abbreviations: CED: convection-enhanced delivery; mCi: millicuries; SPIONs: superparamagnetic iron oxide nanoparticle.

substantial advancements in neurosurgical and imaging technologies, molecular biology (impacting brain tumor classification and diagnosis), and the establishment of concomitant and adjuvant TMZ chemotherapy as the standard of care (Stupp protocol). Consequently, comparisons between modern studies and older data should be made cautiously. In this section, we will focus exclusively on clinical trials involving DDS. While we recognize the significance of other ongoing trials, we have chosen to include only those that have progressed using nanocarriers.

Several trials have studied the clinical potential and complications of CED as an administration route. Two phase I trials involved the intratumoral injection of drug-loaded nanoparticles in GBM patients have recently been completed: IRT-loaded nanoliposomes (NCT02022644) and panobinostat-loaded gold nanoparticles (MTX110, NCT03566199).

A Phase I trial investigated the safety and tolerability of a nanoliposomal IRT formulation administered via CED with real-time MRI guidance in patients with recurrent high-grade glioma [157]. The trial findings reveal prolonged patient survival; however, future studies must include multiple infusions over time using different therapeutic agents and larger drug volumes to ensure optimal tumor coverage.

Another trial evaluated the CED of panobinostat-loaded gold nanoparticles (MTX110, NCT03566199) in patients (2–21 years old) with newly diagnosed diffuse intrinsic pontine glioma (DIPG) [158]. The study demonstrated the feasibility of repeated CED – overall, this approach was well tolerated and may contribute to prolonged survival compared to historical outcomes [158].

The use of liposomes has increased in significance in neuro-oncology due to the impact on pharmacokinetic profiles of the loaded drug and because their distribution within the CNS can be monitored through MRI. For example, Brenner et al. reported the CED of Rhenium (^{186}Re) Obisbemeda (^{186}RNL), and chelated-^{186}Re encapsulated in nanoliposomes to brain tumors and the results of a Phase 1 dose escalation trial (NCT01906385) [159]. This study offered insight into radio-conjugated nanoliposome behavior within the CNS, laying the groundwork for future trials combining theranostic monitoring.

Grauer et al. developed an intracavitary therapeutic platform, NanoPaste, composed of SPIONs – magnetite (Fe_3O_4) cores of around 12 nm in diameter coated with aminosilane – that they applied directly to the walls of the resection cavity in recurrent GBM patients (NCT06271421) [160]. Patients underwent six 1-h hyperthermia sessions in an alternating magnetic field and, if possible, received concurrent fractionated RT at a total dose of 39.6 Gy. Results revealed the upregulation of Caspase-3 and heat shock protein 70 protein levels and the increased infiltration of macrophages with ingested nanoparticles and CD3+ T-cells, suggesting that NanoPaste induces an immunomodulatory effect on GBM. Flow cytometric analysis of freshly prepared tumor cell suspensions revealed increased intracellular ratios of interferon-γ to interleukin-4 in CD4+ and CD8+ memory T cells and the activation of tumor-associated myeloid cells and microglia with upregulation of HLA-DR (Human Leukocyte Antigen – DR isotype) and PD-L1. These data suggest that NanoPaste promotes a more activated and less suppressive GBM TIME. Two patients demonstrated long-lasting treatment responses > 23 months without further therapy; overall, the study reported a median survival of 8.3 months.

Jonas et al. developed small (6 mm × 0.7 mm), biocompatible intratumoral microdevices (mIMDs) that can be directly implanted into the tumor at the onset of surgery (NCT04135807) [161]. mIMDs remain in place throughout tumor resection but become removed along with the final portion of the tumor at the close of the operation. This strategy enables a 2–3 h window of localized drug exposure within the intact tumor microenvironment. During this period, IMDs release nanodoses of multiple drugs (~1/100,000th of the dose) in a spatially segregated manner, ensuring minimal overlap between drug diffusion zones but achieving therapeutically relevant concentrations in the immediate tissue vicinity (0.5–1 mm from the release site). Preliminary evidence suggests that drug effect readouts from IMDs at intratumoral nanodose levels correlate with systemic treatment responses observed in GBM patients. Further studies are necessary to understand the impact of this treatment.

Emerging clinical trials demonstrate the potential of localized DDSs for GBM, with some strategies reporting enhanced drug targeting and immune activation; however, improvements in patient survival remain modest. Continued research must optimize delivery methods, enable repeat dosing, and integrate these systems with standard therapies in larger, well-controlled trials.

5. Conclusion

Despite advancements in neurosurgery, imaging technologies, radiation protocols, and therapeutic strategies, long-term solutions to prevent GBM recurrence remain much needed. Advancements in DDS design – including dimension, surface charge, chemistry, and brain tumor-specific targeting ligands – have shown tremendous potential for improving brain parenchyma penetration [41,86]; however, the development of novel soft-matter biomaterials capable of infiltrating the GBM mass and targeting infiltrative cells remains a crucial need, always keeping in mind scalability. These strategies should be complemented by advanced models for testing these novel DDS, including in vitro, ex vivo, and in vivo approaches, along with the exploration of new therapeutics to validate their effectiveness. In the next section, we will discuss a few challenges of these challenges.

6. Future perspectives

Effective brain penetration strategies remain a significant hurdle for treating unresectable GBM, where the dense stroma hinders DDS diffusion [91,92,103]. In resected GBM, these strategies must be coupled with implants and scaffolds; additionally, next-generation localized DDS for GBM must be designed with surgical applicability, ensuring ease of use and rapid application by neurosurgeons. This highlights the importance of an interdisciplinary team, including surgeons, engineers, clinicians, drug delivery and biomaterial scientists, pharmacists, and analytical chemists, in designing pre-clinical studies to tackle GBM [41].

A significant limitation remains in the currently employed rodent pre-clinical models, which may not accurately reflect the true infiltrative clinical nature of GBM. Rodent xenograft and allograft orthotopic brain tumor models represent the most common means of testing DDS for GBM applied via CED and surgical resection; however, researchers might consider two points. First, humanized GBM models hold more clinical relevance; however, most studies have involved immunocompromised mice or rats, which remain unsuitable for studying the TIME and immunotherapeutic treatment strategies. Second, the ability of GBM cells to invade and diffuse from the tumor mass into the brain parenchyma varies across different GBM models [162,163]. In this context, spontaneously occurring de novo GBM in canines offers a potential alternative for evaluating localized drug delivery for infiltrative disease treatment; however, these studies tend to lack an adequate statistical number of animals and proper comparison with the standard of care, which reduces the impact on clinical translation. Even with prospective veterinary research, significant challenges remain in establishing effective treatment and control arms. Ultimately, de novo transgenic GBM syngeneic rodent models, which better replicate infiltration, may become the most reliable pre-clinical models for predicting phase I safety and phase II response in GBM clinical trials [163].

Next-generation localized DDS for GBM must also consider the rational design or repurposing of molecularly targeted drug compounds based on integrative omics of infiltrative GBM. Much of the current research focuses on understanding the underlying mechanisms of tumor regrowth and treatment resistance to identify therapeutic targets for both monotherapies and combinatory approaches. Emerging technologies, such as FUS, are being explored in preclinical in vitro and in vivo models to stimulate immune responses and transiently disrupt the blood-brain barrier, thereby enhancing the delivery of traditional therapeutics and novel therapies, including immunotherapeutics (such as chimeric antigen receptor T-cell therapy, immunomodulators, and immune checkpoint inhibitors) to the tumor site [9,164]. Although non-chemical therapies have significantly advanced GBM treatment, none have provided a definitive path to a cure [165]; notably, the post-operative interval before initiating RT and chemotherapy offers a strategic window for delivering localized, first-line therapies directly to the resection cavity, potentially improving outcomes by targeting residual tumor cells before systemic treatment begins [166]. Personalized genomics may guide individualized drug delivery, but they do introduce new challenges for clinical trial design; furthermore, a deeper understanding of the molecular and cellular aspects of the brain microenvironment within the GBM infiltrative margin will allow for the creation of more clinically accurate DDS defined as “neuro-nanotechnology” [167].

Finally, the scalability of a DDS for clinical applications, good manufacturing practice-compliant characterization, and early engagement with regulatory agencies should be considered early in the pre-clinical research phase [168]. Many DDSs are likely to be regulated as drugs due to the lack of medicinal value from a drug-free DDS. If the many challenges discussed in this review are addressed in the coming years, there exist reasons to be optimistic that localized delivery of high therapeutic concentrations of drug combinations could significantly extend survival while minimizing or avoiding dose-limiting systemic toxicities.

Acknowledgments

We thank Dr. Stuart P. Atkinson for his help with manuscript editing. The graphical abstract was made using Biorender (license purchased by the University of Padova).

Author contribution

Cristiano Pesce: Writing – original draft, review & editing, conceptualization; Giulia Rodella: Writing – original draft, review & editing, conceptualization; Agnese Fragassi: Writing – review & editing, Conceptualization; Mariangela Garofalo: review & editing; Stefano Salmaso: review & editing; Paolo Caliceti: review & editing; Bernard Gallez: Writing – review & editing, Supervision, Conceptualization; Alessio Malfanti: Writing – original draft, review & editing, conceptualization, supervision, resources.

Disclosure statement

The authors have no relevant affiliations or financial involvement with any organization or entity with a financial interest in or financial conflict with the subject matter or materials discussed in the manuscript. This includes employment, consultancies, honoraria, stock ownership or options, expert testimony, grants or patents received or pending, or royalties.

Funding

G.R. is supported by the EuroNanoMed III Consortium RAIN (RadioActivated Immunomodulating Niches) fellowship. M.G.thanks the Ministry of Education, University and Research – PRIN funding scheme, "EVs-like nanoparticles carrying oncolytic viruses as a novel platform for cancer treatment (EVCARE)" (MUR 2022H3AM7R). S.S. thanks the MIMIT for the support (TALISMAN, F/350078/01–05/X60 - CUP B79J23005390005) through the scheme "Accordi per l'innovazione 2022– Bando 2 (DD 14/11/2022)". A.M thanks the following funding agencies for their generous support: the European Research Council (ERC) Starting Grant (grant agreement no.101163931-GLIOMERS); University of Padova (Italy) (STARS StG 2023, Grant Number: MALF_STARS_MUR24_01 and Progetti di Ateneo, 2024, PRIDJ no MALF_BIRD24_02).

Writing assistance

No writing assistance was utilized in the production of this manuscript.

Reviewer disclosure

Peer reviewers on this manuscript have no relevant financial or other relationships to disclose.

References

Papers of special note have been highlighted as either of interest (•) or of considerable interest (••) to readers.

1. Weller M, Wen PY, Chang SM, et al. Glioma. Nat Rev Dis Primers. 2024;10(1):33. doi: 10.1038/s41572-024-00516-y
2. Louis DN, Perry A, Wesseling P, et al. The 2021 WHO classification of tumors of the central nervous system: a summary. Neuro Oncol. 2021;23(8):1231–1251. doi: 10.1093/neuonc/noab106
3. Ostrom QT, Shoaf ML, Cioffi G, et al. National-level overall survival patterns for molecularly-defined diffuse glioma types in the United States. Neuro Oncol. 2023;25(4):799–807. doi: 10.1093/neuonc/noac198
4. Wang F, Zheng Z, Guan J, et al. Identification of a panel of genes as a prognostic biomarker for glioblastoma. EBioMedicine. 2018;37:68–77. doi: 10.1016/j.ebiom.2018.10.024
5. Thakkar JP, Dolecek TA, Horbinski C, et al. Epidemiologic and molecular prognostic review of glioblastoma. Cancer Epidemiol Biomarker Prev. 2014;23(10):1985–1996. doi: 10.1158/1055-9965.EPI-14-0275
6. Xiao D, Yan C, Li D, et al. National brain tumour registry of China (NBTRC) statistical report of primary brain tumours diagnosed in China in years 2019–2020. Lancet Reg health–West Pac. 2023;34:100715. doi: 10.1016/j.lanwpc.2023.100715
7. Pöhlmann J, Weller M, Marcellusi A, et al. High costs, low quality of life, reduced survival, and room for improving treatment: an analysis of burden and unmet needs in glioma. Front Oncol. 2024;14:1368606. doi: 10.3389/fonc.2024.1368606
8. Yeini E, Ofek P, Albeck N, et al. Targeting glioblastoma: advances in drug delivery and novel therapeutic approaches. Adv Ther. 2021;4(1):2000124. doi: 10.1002/adtp.202000124
9. Bausart M, Préat V, Malfanti A. Immunotherapy for glioblastoma: the promise of combination strategies. J Exp Clin Cancer Res. 2022;41(1):1–22. doi: 10.1186/s13046-022-02251-2
10. Diksin M, Smith SJ, Rahman R. The molecular and phenotypic basis of the glioma invasive perivascular niche. Int J Mol Sci. 2017;18(11):2342. doi: 10.3390/ijms18112342
11. Sottoriva A, Spiteri I, Piccirillo SG, et al. Intratumor heterogeneity in human glioblastoma reflects cancer evolutionary dynamics. Proc Natl Acad Sci USA. 2013;110(10):4009–4014. doi: 10.1073/pnas.1219747110
12. Gimple RC, Bhargava S, Dixit D, et al. Glioblastoma stem cells: lessons from the tumor hierarchy in a lethal cancer. Genes Dev. 2019;33(11–12):591–609. doi: 10.1101/gad.324301.119
13. Jadoon SS, Ilyas U, Zafar H, et al. Genomic and epigenomic features of glioblastoma multiforme and its biomarkers. J Oncol. 2022;2022(1):1–16. doi: 10.1155/2022/4022960
14. Stupp R, Brada M, Van Den Bent M, et al. High-grade glioma: ESMO clinical practice guidelines for diagnosis, treatment and follow-up. Ann Oncol. 2014;25:iii93–iii101. doi: 10.1093/annonc/mdu050
15. Stupp R, Mason WP, Van Den Bent MJ, et al. Radiotherapy plus concomitant and adjuvant temozolomide for glioblastoma. N Engl J Med. 2005;352(10):987–996. doi: 10.1056/NEJMoa043330
16. Stupp R, Taillibert S, Kanner AA, et al. Maintenance therapy with tumor-treating fields plus temozolomide vs temozolomide alone for glioblastoma: a randomized clinical trial. JAMA. 2015;314(23):2535–2543. doi: 10.1001/jama.2015.16669
17. Bernstock JD, Gary SE, Klinger N, et al. Standard clinical approaches and emerging modalities for glioblastoma imaging. neuro-Oncol Adv. 2022;4(1):vdac080. doi: 10.1093/noajnl/vdac080
18. Youngblood MW, Stupp R, Sonabend AM. Role of resection in glioblastoma management. Neurosurg Clinics. 2021;32(1):9–22. doi: 10.1016/j.nec.2020.08.002
19. Coburger J, Wirtz CR. Fluorescence guided surgery by 5-ALA and intraoperative MRI in high grade glioma: a systematic review. J Neurooncol. 2019;141(3):533–546. doi: 10.1007/s11060-018-03052-4
20. Pallud J, Rigaux-Viode O, Corns R, et al. Direct electrical bipolar electrostimulation for functional cortical and subcortical cerebral mapping in awake craniotomy Practical Considerations. Neurochirurgie. 2017;63(3):164–174. doi: 10.1016/j.neuchi.2016.08.009
21. De Witt Hamer PC, Robles SG, Zwinderman AH, et al. Impact of intraoperative stimulation brain mapping on glioma surgery outcome: a meta-analysis. J Clin Oncol. 2012;30(20):2559–2565. doi: 10.1200/JCO.2011.38.4818
22. Alderson P, Roberts I. Corticosteroids for acute traumatic brain injury. Cochrane Database System Rev. 2005;2005(1). doi: 10.1002/14651858.CD000196.pub2
23. Walbert T, Harrison RA, Schiff D, et al. SNO and EANO practice guideline update: anticonvulsant prophylaxis in patients with newly diagnosed brain tumors. Neuro Oncol. 2021;23(11):1835–1844. doi: 10.1093/neuonc/noab152
24. Cabrera AR, Kirkpatrick JP, Fiveash JB, et al. Radiation therapy for glioblastoma: executive summary of an American society for radiation oncology evidence-based clinical practice guideline. Pract Radiat Oncol. 2016;6(4):217–225. doi: 10.1016/j.prro.2016.03.007
25. Minniti G, Niyazi M, Alongi F, et al. Current status and recent advances in reirradiation of glioblastoma. Radiat Oncol. 2021;16(1):1–14. doi: 10.1186/s13014-021-01767-9
26. Hynes PR, Das JM. Stereotactic radiosurgery (SRS) and stereotactic body radiotherapy (SBRT). In: StatPearls. StatPearls Publishing; 2023.
27. Sheline GE, Wara WM, Smith V. Therapeutic irradiation and brain injury. Int J Radiat Oncol* Biol* Phys. 1980;6(9):1215–1228. doi: 10.1016/0360-3016(80)90175-3
28. Barisano G, Bergamaschi S, Acharya J, et al. Complications of radiotherapy and radiosurgery in the brain and spine. Neurographics. 2018;8(3):167–187 . doi: 10.3174/ng.1700066
29. Ortiz R, Perazzoli G, Cabeza L, et al. Temozolomide: an updated overview of resistance mechanisms, nanotechnology advances and clinical applications. Curr Neuropharmacol. 2021;19(4):513–537. doi: 10.2174/1570159X18666200626204005
30. Wu H, Gao W, Chen P, et al. Research progress of drug resistance mechanism of temozolomide in the treatment of glioblastoma. Heliyon. 2024;10(21):e39984. doi: 10.1016/j.heliyon.2024.e39984

31. Singh N, Miner A, Hennis L, et al. Mechanisms of temozolomide resistance in glioblastoma-a comprehensive review. Cancer Drug Resist. 2021;4(1):17. doi: 10.20517/cdr.2020.79
32. Kelly K, Sacapano M, Prosolovich K, et al. Blood brain barrier permeability to temozolomide. Cancer Res. 2005;65(9 Supplement):330.
33. Cordner R, Black KL, Wheeler CJ. Exploitation of adaptive evolution in glioma treatment. CNS Oncol. 2013;2(2):171–179. doi: 10.2217/cns.12.46
34. Wang P, Liao B, Gong S, et al. Temozolomide promotes glioblastoma stemness expression through senescence-associated reprogramming via HIF1α/HIF2α regulation. Cell Death Dis. 2025;16(1):317. doi: 10.1038/s41419-025-07617-w
35. Wu W, Klockow JL, Zhang M, et al. Glioblastoma multiforme (GBM): an overview of current therapies and mechanisms of resistance. Pharmacol Res. 2021;171:105780. doi: 10.1016/j.phrs.2021.105780
36. Tesileanu CMS, Sanson M, Wick W, et al. Temozolomide and radiotherapy versus radiotherapy alone in patients with glioblastoma, IDH-wildtype: post hoc analysis of the EORTC randomized phase III CATNON trial. Clin Cancer Res. 2022;28(12):2527–2535. doi: 10.1158/1078-0432.CCR-21-4283
37. Perry J, Chambers A, Spithoff K, et al. Gliadel wafers in the treatment of malignant glioma: a systematic review. Curr Oncol. 2007;14(5):189. doi: 10.3747/co.2007.147
38. Bregy A, Shah AH, Diaz MV, et al. The role of Gliadel wafers in the treatment of high-grade gliomas. Expert Rev Anticancer Ther. 2013;13(12):1453–1461. doi: 10.1586/14737140.2013.840090
39. Chew SA, Danti S. Biomaterial-based implantable devices for cancer therapy. Adv Healthc Mater. 2017;6(2):1600766. doi: 10.1002/adhm.201600766
40. Ashby LS, Smith KA, Stea B. Gliadel wafer implantation combined with standard radiotherapy and concurrent followed by adjuvant temozolomide for treatment of newly diagnosed high-grade glioma: a systematic literature review. World J Surg Onc. 2016;14(1):1–15. doi: 10.1186/s12957-016-0975-5
41. Bastiancich C, Malfanti A, Préat V, et al. Rationally designed drug delivery systems for the local treatment of resected glioblastoma. Adv Drug Deliv Rev. 2021;177:113951. doi: 10.1016/j.addr.2021.113951
42. Lillehei KO, Kalkanis SN, Liau LM, et al. Rationale and design of the 500-patient, 3-year, and prospective vigilant ObservatIon of GIladeL WAfer ImplaNT registry. CNS Oncol. 2017;7(2):CNS08. doi: 10.2217/cns-2017-0036
43. Cohen MH, Shen YL, Keegan P, et al. FDA drug approval summary: bevacizumab (Avastin®) as treatment of recurrent glioblastoma multiforme. Oncologist. 2009;14(11):1131–1138. doi: 10.1634/theoncologist.2009-0121
44. Winograd E, Germano I, Wen P, et al. Congress of neurological surgeons systematic review and evidence-based guidelines update on the role of targeted therapies and immunotherapies in the management of progressive glioblastoma. J Neurooncol. 2022;158(2):265–321.
45. Vasudev NS, Reynolds AR. Anti-angiogenic therapy for cancer: current progress, unresolved questions and future directions. Angiogenesis. 2014;17(3):471–494. doi: 10.1007/s10456-014-9420-y
46. Ghiaseddin A, Peters KB. Use of bevacizumab in recurrent glioblastoma. CNS Oncol. 2015;4(3):157–169. doi: 10.2217/cns.15.8
47. Guo X, Yang X, Wu J, et al. Tumor-treating fields in glioblastomas: past, present, and future. Cancers (Basel). 2022;14(15):3669. doi: 10.3390/cancers14153669
48. Rominiyi O, Vanderlinden A, Clenton SJ, et al. Tumour treating fields therapy for glioblastoma: current advances and future directions. Br J Cancer. 2021;124(4):697–709. doi: 10.1038/s41416-020-01136-5
49. Davies AM, Weinberg U, Palti Y. Tumor treating fields: a new frontier in cancer therapy. Ann N Y Acad Sci. 2013;1291(1):86–95. doi: 10.1111/nyas.12112
50. Zhu J-J, Demireva P, Kanner AA, et al. Health-related quality of life, cognitive screening, and functional status in a randomized phase III trial (EF-14) of tumor treating fields with temozolomide compared to temozolomide alone in newly diagnosed glioblastoma. J Neurooncol. 2017;135(3):545–552. doi: 10.1007/s11060-017-2601-y
51. Ballo M, Conlon P, Lavy-Shahaf G, et al. Tumor treating fields (TTFields) for newly diagnosed glioblastoma in the real world: a systematic review and survival meta-analysis. Int J Radiat Oncol Biol Phys. 2023;117(2):e85. doi: 10.1016/j.ijrobp.2023.06.837
52. Brem S, Tyler B, Li K, et al. Local delivery of temozolomide by biodegradable polymers is superior to oral administration in a rodent glioma model. Cancer Chemother Pharmacol. 2007;60(5):643–650. doi: 10.1007/s00280-006-0407-2
53. van Solinge TS, Niela Nd L, Chiocca EA, et al. Advances in local therapy for glioblastoma—taking the fight to the tumour. Nat Rev Neurol. 2022;18(4):221–236. doi: 10.1038/s41582-022-00621-0
•• **This is a cohomprensive review that discuss the recent clinical trails combining DDS and local appraoches.**
54. Ius T, Somma T, Pasqualetti F, et al. Local therapy in glioma: an evolving paradigm from history to horizons. Oncol Lett. 2024;28(3):440. doi: 10.3892/ol.2024.14573
55. Ellis JA, Banu M, Hossain SS, et al. Reassessing the role of intra-arterial drug delivery for glioblastoma multiforme treatment. J Drug Deliv. 2015;2015(1):1–15. doi: 10.1155/2015/405735
56. Yuan F, Salehi HA, Boucher Y, et al. Vascular permeability and microcirculation of gliomas and mammary carcinomas transplanted in rat and mouse cranial windows. Cancer Res. 1994;54(17):4564–4568.
57. Conq J, Joudiou N, Ucakar B, et al. Assessment of hyperosmolar blood–brain barrier opening in glioblastoma via histology with Evans Blue and DCE-MRI. Biomedicines. 2023;11(7):1957. doi: 10.3390/biomedicines11071957
58. Pinkiewicz M, Pinkiewicz M, Walecki J, et al. A systematic review on intra-arterial cerebral infusions of chemotherapeutics in the treatment of glioblastoma multiforme: the state-of-the-art. Front Oncol. 2022;12:950167. doi: 10.3389/fonc.2022.950167
59. Jain RK. Delivery of novel therapeutic agents in tumors: physiological barriers and strategies. J Natl Cancer Inst. 1989;81(8):570. doi: 10.1093/jnci/81.8.570
60. Jahangiri A, Chin AT, Flanigan PM, et al. Convection-enhanced delivery in glioblastoma: a review of preclinical and clinical studies. J Neurosurg. 2017;126(1):191–200. doi: 10.3171/2016.1.JNS151591
61. Mokarram N, Case A, Hossainy NN, et al. Device-assisted strategies for drug delivery across the blood-brain barrier to treat glioblastoma. Commun Mater. 2025;6(1):5. doi: 10.1038/s43246-024-00721-y
62. Lee I, Kalkanis S, Hadjipanayis CG. Stereotactic laser interstitial thermal therapy for recurrent high-grade gliomas. Neurosurgery. 2016;79(Supplement 1):S24–S34. doi: 10.1227/NEU.0000000000001443
63. Holste KG, Orringer DA. Laser interstitial thermal therapy. neuro-Oncol Adv. 2020;2(1):vdz035. doi: 10.1093/noajnl/vdz035
64. Seaton MP, Schmidt JC, Brown NJ, et al. Contemporary applications of laser interstitial thermal therapy: a comprehensive systematic review. World Neurosurg. 2024;193:356–372. doi: 10.1016/j.wneu.2024.10.022
65. Kamath AA, Friedman DD, Akbari SHA, et al. Glioblastoma treated with magnetic resonance imaging-guided laser interstitial thermal therapy: safety, efficacy, and outcomes. Neurosurg. 2019;84(4):836–843. doi: 10.1093/neuros/nyy375
66. Chen C, Lee I, Tatsui C, et al. Laser interstitial thermotherapy (LITT) for the treatment of tumors of the brain and spine: a brief review. J Neurooncol. 2021;151(3):429–442. doi: 10.1007/s11060-020-03652-z
67. Mohammadi AM, Hawasli AH, Rodriguez A, et al. The role of laser interstitial thermal therapy in enhancing progression-free survival of difficult-to-access high-grade gliomas: a multicenter study. Cancer Med. 2014;3(4):971–979. doi: 10.1002/cam4.266
68. Bérard C, Truillet C, Larrat B, et al. Anticancer drug delivery by focused ultrasound-mediated blood-brain/tumor barrier disruption for glioma therapy: from benchside to bedside. Pharmacol Ther. 2023;250:108518. doi: 10.1016/j.pharmthera.2023.108518

69. Bunevicius A, McDannold NJ, Golby AJ. Focused ultrasound strategies for brain tumor therapy. Operative Surg. 2020;19(1):9–18. doi: 10.1093/ons/opz374
70. Guthkelch A, Carter L, Cassady J, et al. Treatment of malignant brain tumors with focused ultrasound hyperthermia and radiation: results of a phase I trial. J neuro-Oncol. 1991;10(3):271–284. doi: 10.1007/BF00177540
71. Young JS, Semonche A, Morshed RA, et al. Focused ultrasound therapy as a strategy for improving glioma treatment. J Neurosurg. 2025;142(6):1635–1644. doi: 10.3171/2024.9.JNS24721
72. Tavakkoli Yaraki M, Liu B, Tan YN. Emerging strategies in enhancing singlet oxygen generation of nano-photosensitizers toward advanced phototherapy. Nano-Micro Lett. 2022;14(1):123. doi: 10.1007/s40820-022-00856-y
73. Lu Y, Sun W, Du J, et al. Immuno-photodynamic therapy (IPDT): organic photosensitizers and their application in cancer ablation. Jacs Au. 2023;3(3):682–699. doi: 10.1021/jacsau.2c00591
74. Aebisher D, Przygórzewska A, Myśliwiec A, et al. Current photodynamic therapy for glioma treatment: an update. Biomedicines. 2024;12(2):375. doi: 10.3390/biomedicines12020375
75. Stummer W, Pichlmeier U, Meinel T, et al. Fluorescence-guided surgery with 5-aminolevulinic acid for resection of malignant glioma: a randomised controlled multicentre phase III trial. Lancet Oncol. 2006;7(5):392–401. doi: 10.1016/S1470-2045(06)70665-9
76. Stepp H, Stummer W. 5-ALA in the management of malignant glioma. Lasers Surg Med. 2018;50(5):399–419. doi: 10.1002/lsm.22933
77. Pena ES, Graham-Gurysh EG, Bachelder EM, et al. Design of biopolymer-based interstitial therapies for the treatment of glioblastoma. Int J Mol Sci. 2021;22(23):13160. doi: 10.3390/ijms222313160
78. Magill ST, Choy W, Nguyen MP, et al. Ommaya reservoir insertion: a technical note. Cureus. 2020;12(4). doi: 10.7759/cureus.7731
79. Cha GD, Jung S, Choi SH, et al. Local drug delivery strategies for glioblastoma treatment. Brain Tumor Res Treat. 2022;10(3):151–157. doi: 10.14791/btrt.2022.0017
80. Hauck M, Hellmold D, Kubelt C, et al. Localized drug delivery systems in high-grade glioma therapy—from construction to application. Adv Ther. 2022;5(8):2200013. doi: 10.1002/adtp.202200013
81. Stewart SA, Domínguez-Robles J, Donnelly RF, et al. Implantable polymeric drug delivery devices: classification, manufacture, materials, and clinical applications. Polymers. 2018;10(12):1379. doi: 10.3390/polym10121379
82. Mohtaram NK, Montgomery A, Willerth SM. Biomaterial-based drug delivery systems for the controlled release of neurotrophic factors. Biomed Mater. 2013;8(2):022001. doi: 10.1088/1748-6041/8/2/022001
83. Vargová L, Homola A, Zámečník J, et al. Diffusion parameters of the extracellular space in human gliomas. Glia. 2003;42(1):77–88. doi: 10.1002/glia.10204
84. Heldin C-H, Rubin K, Pietras K, et al. High interstitial fluid pressure—an obstacle in cancer therapy. Nat Rev Cancer. 2004;4(10):806–813. doi: 10.1038/nrc1456
85. Sun B, Li R, Ji N, et al. Brain-targeting drug delivery systems: the state of the art in treatment of glioblastoma. Mater Today Bio. 2025;30:101443. doi: 10.1016/j.mtbio.2025.101443
86. Song E, Gaudin A, King AR, et al. Surface chemistry governs cellular tropism of nanoparticles in the brain. Nat Commun. 2017;8(1):15322. doi: 10.1038/ncomms15322
•• **This is an interesting work were it discuss how the biomaterial has a role in the biodistribition in the brain and how dis can be used to tackle inoperable GBM.**
87. Seo Y-E, Bu T, Saltzman WM. Nanomaterials for convection-enhanced delivery of agents to treat brain tumors. Curr Opin Biomed Eng. 2017;4:1–12. doi: 10.1016/j.cobme.2017.09.002
88. Neeves KB, Sawyer AJ, Foley CP, et al. Dilation and degradation of the brain extracellular matrix enhances penetration of infused polymer nanoparticles. Brain Res. 2007;1180:121–132. doi: 10.1016/j.brainres.2007.08.050
89. Perrin SL, Samuel MS, Koszyca B, et al. Glioblastoma heterogeneity and the tumour microenvironment: implications for preclinical research and development of new treatments. Biochem Soc Trans. 2019;47(2):625–638. doi: 10.1042/BST20180444
90. Yeini E, Ofek P, Pozzi S, et al. P-selectin axis plays a key role in microglia immunophenotype and glioblastoma progression. Nat Commun. 2021;12(1):1912. doi: 10.1038/s41467-021-22186-0
• **The authors show that P-selectin mediates microglia-enhanced GB proliferation and invasion by altering microglia/macrophages activation state and might represent a target for future immunotherapeutic approaches for several DDSs.**
91. Nance EA, Woodworth GF, Sailor KA, et al. A dense poly (ethylene glycol) coating improves penetration of large polymeric nanoparticles within brain tissue. Sci Transl Med. 2012;4(149):ra14919–ra19. doi: 10.1126/scitranslmed.3003594
•• **This is a first report of using PEG as brain penetration enhancer after local treatment.**
92. Nance E, Zhang C, Shih T-Y, et al. Brain-penetrating nanoparticles improve paclitaxel efficacy in malignant glioma following local administration. ACS Nano. 2014;8(10):10655–10664. doi: 10.1021/nn504210g
93. McConville C, Lastakchi S, Al Amri A, et al. Local delivery of irinotecan to recurrent GBM patients at reoperation offers a safe route of administration. Cancers (Basel). 2024;16(17):3008. doi: 10.3390/cancers16173008
94. Sawyer AJ, Saucier-Sawyer JK, Booth CJ, et al. Convection-enhanced delivery of camptothecin-loaded polymer nanoparticles for treatment of intracranial tumors. Drug Deliv Transl Res. 2011;1(1):34–42. doi: 10.1007/s13346-010-0001-3
95. Arshad A, Yang B, Bienemann AS, et al. Convection-enhanced delivery of carboplatin PLGA nanoparticles for the treatment of glioblastoma. PLOS ONE. 2015;10(7):e0132266. doi: 10.1371/journal.pone.0132266
96. Bausart M, Rodella G, Dumont M, et al. Combination of local immunogenic cell death-inducing chemotherapy and DNA vaccine increases the survival of glioblastoma-bearing mice. Nanomed: Nanotechnol Biol Med. 2023;50:102681. doi: 10.1016/j.nano.2023.102681
97. Mastorakos P, Zhang C, Berry S, et al. Highly PEGylated DNA nanoparticles provide uniform and widespread gene transfer in the brain. Adv Healthcare Mater. 2015;4(7):1023–1033. doi: 10.1002/adhm.201400800
98. Mastorakos P, Song E, Zhang C, et al. Biodegradable DNA nanoparticles that provide widespread gene delivery in the brain. Small. 2016;12(5):678–685. doi: 10.1002/smll.201502554
99. Martins C, Araújo M, Malfanti A, et al. Stimuli-responsive multifunctional nanomedicine for enhanced glioblastoma chemotherapy augments multistage blood-to-brain trafficking and tumor targeting. Small. 2023;19(22):2300029. doi: 10.1002/smll.202300029
100. Barrios-Esteban S, Reimóndez-Troitiño S, Cabezas-Sainz P, et al. Protamine-based Nanotherapeutics for gene delivery to glioblastoma cells. Mol Pharm. 2025;22(5):2466–2481. doi: 10.1021/acs.molpharmaceut.4c01269
101. Ekladious I, Colson YL, Grinstaff MW. Polymer–drug conjugate therapeutics: advances, insights and prospects. Nat Rev Drug Discov. 2019;18(4):273–294. doi: 10.1038/s41573-018-0005-0
102. Rodriguez-Otormin F, Duro-Castano A, Conejos-Sánchez I, et al. Envisioning the future of polymer therapeutics for brain disorders. WIREs Nanomed Nanobiotechnol. 2019;11(1):e1532. doi: 10.1002/wnan.1532
103. Zhang C, Nance EA, Mastorakos P, et al. Convection enhanced delivery of cisplatin-loaded brain penetrating nanoparticles cures malignant glioma in rats. J Control Release. 2017;263:112–119. doi: 10.1016/j.jconrel.2017.03.007
104. Dosta P, Dion MZ, Prado M, et al. Matrix metalloproteinase-and pH-sensitive nanoparticle system enhances drug retention and penetration in glioblastoma. ACS Nano. 2024;18(22):14145–14160. doi: 10.1021/acsnano.3c03409
105. Catania G, Rodella G, Vanvarenberg K, et al. Combination of hyaluronic acid conjugates with immunogenic cell death inducer and

CpG for glioblastoma local chemo-immunotherapy elicits an immune response and induces long-term survival. Biomaterials. 2023;294:122006. doi: 10.1016/j.biomaterials.2023.122006
106. Malfanti A, Catania G, Degros Q, et al. Design of bio-responsive hyaluronic acid–doxorubicin conjugates for the local treatment of glioblastoma. Pharmaceutics. 2022;14(1):124. doi: 10.3390/pharmaceutics14010124
107. Rodella G, Ma Z, Ucakar B, et al. Repurposing chemotherapeutics in a hyaluronic acid-conjugate combination treatment approach for the local immunomodulation of the glioblastoma microenvironment. Int J Pharm. 2025;676:125612. doi: 10.1016/j.ijpharm.2025.125612
108. Chellen T, Bausart M, Maus P, et al. In situ administration of STING-activating hyaluronic acid conjugate primes anti-glioblastoma immune response. Mater Today Bio. 2024;26:101057. doi: 10.1016/j.mtbio.2024.101057
109. Dasgupta A, May J-N, Klinkenberg G, et al. Multidrug micelles and sonopermeation for chemotherapy co-delivery to brain tumors. J Control Release. 2025;380:818–828. doi: 10.1016/j.jconrel.2025.02.018
110. Clavreul A, Roger E, Pourbaghi-Masouleh M, et al. Development and characterization of sorafenib-loaded lipid nanocapsules for the treatment of glioblastoma. Drug Deliv. 2018;25(1):1756–1765. doi: 10.1080/10717544.2018.1507061
111. Lollo G, Vincent M, Ullio-Gamboa G, et al. Development of multifunctional lipid nanocapsules for the co-delivery of paclitaxel and CpG-ODN in the treatment of glioblastoma. Int J Pharm. 2015;495(2):972–980. doi: 10.1016/j.ijpharm.2015.09.062
112. Kadiyala P, Li D, Nuñez FM, et al. High-density lipoprotein-mimicking nanodiscs for chemo-immunotherapy against glioblastoma multiforme. ACS Nano. 2019;13(2):1365–1384. doi: 10.1021/acsnano.8b06842
113. Halseth TA, Mujeeb AA, Liu L, et al. HDL nanodiscs loaded with Liver X receptor agonist decreases tumor burden and mediates long-term survival in mouse glioma model. Small. 2025;21(20):2307097. doi: 10.1002/smll.202307097
• **In this article, the authors target cholesterol metabolism to induce cancer cell death in combination with and CpG oligonucleotides in the context of local GBM treatment, paving the way for further combination therapies (e.g. radiation).**
114. Guo X, Zhou S, Yang Z, et al. Cholesterol metabolism and its implication in glioblastoma therapy. J Cancer. 2022;13(6):1745. doi: 10.7150/jca.63609
115. Cohen ZR, Ramishetti S, Peshes-Yaloz N, et al. Localized RNAi therapeutics of chemoresistant grade IV glioma using hyaluronan-grafted lipid-based nanoparticles. ACS Nano. 2015;9(2):1581–1591. doi: 10.1021/nn506248s
116. Bi D, Unthan DM, Hu L, et al. Polysarcosine-based lipid formulations for intracranial delivery of mRNA. J Control Release. 2023;356:1–13. doi: 10.1016/j.jconrel.2023.02.021
117. Saito R, Krauze MT, Noble CO, et al. Tissue affinity of the infusate affects the distribution volume during convection-enhanced delivery into rodent brains: implications for local drug delivery. J Neurosci Methods. 2006;154(1–2):225–232. doi: 10.1016/j.jneumeth.2005.12.027
118. Saito R, Krauze MT, Noble CO, et al. Convection-enhanced delivery of ls-TPT enables an effective, continuous, low-dose chemotherapy against malignant glioma xenograft model. Neuro Oncol. 2006;8(3):205–214. doi: 10.1215/15228517-2006-001
119. Drummond DC, Noble CO, Guo Z, et al. Development of a highly active nanoliposomal irinotecan using a novel intraliposomal stabilization strategy. Cancer Res. 2006;66(6):3271–3277. doi: 10.1158/0008-5472.CAN-05-4007
120. Joshi S, Cooke JR, Chan DK, et al. Liposome size and charge optimization for intraarterial delivery to gliomas. Drug Deliv Transl Res. 2016;6(3):225–233. doi: 10.1007/s13346-016-0294-y
121. Grzegorzewski J, Michalak M, Wołoszczuk M, et al. Nanotherapy of glioblastoma—where hope grows. Int J Mol Sci. 2025;26(5):1814. doi: 10.3390/ijms26051814
122. Maier-Hauff K, Ulrich F, Nestler D, et al. Efficacy and safety of intratumoral thermotherapy using magnetic iron-oxide nanoparticles combined with external beam radiotherapy on patients with recurrent glioblastoma multiforme. J Neurooncol. 2011;103(2):317–324. doi: 10.1007/s11060-010-0389-0
123. Wu M, Chen W, Chen Y, et al. Focused ultrasound-augmented delivery of biodegradable multifunctional nanoplatforms for imaging-guided brain tumor treatment. Adv Sci. 2018;5(4):1700474. doi: 10.1002/advs.201700474
124. Huang X, Gao L, Ge W, et al. An ultrasound-activated piezoelectric sonosensitizer enhances mitochondrial depolarization for effective treatment of orthotopic glioma. Acta Biomater. 2024;190:435–446. doi: 10.1016/j.actbio.2024.10.051
125. Alghamdi M, Gumbleton M, Newland B. Local delivery to malignant brain tumors: potential biomaterial-based therapeutic/adjuvant strategies. Biomater Sci. 2021;9(18):6037–6051. doi: 10.1039/D1BM00896J
126. Shaha S, Rodrigues D, Mitragotri S. Locoregional drug delivery for cancer therapy: preclinical progress and clinical translation. J Control Release. 2024;367:737–767. doi: 10.1016/j.jconrel.2024.01.072
127. Anderson AR, Segura T. Injectable biomaterials for treatment of glioblastoma. Adv Mater Inter. 2020;7(20):2001055. doi: 10.1002/admi.202001055
128. Kisby T, Borst GR, Coope DJ, et al. Targeting the glioblastoma resection margin with locoregional nanotechnologies. Nat Rev Clin Oncol. 2025;22(7):517–537. doi: 10.1038/s41571-025-01020-2
•• **This is a cohomprensive review that discuss the recent clinical trails combining DDS and local appraoches in the context of resected GBM.**
129. Gao W, Zhang Y, Zhang Q, et al. Nanoparticle-hydrogel: a hybrid biomaterial system for localized drug delivery. Ann Biomed Eng. 2016;44(6):2049–2061. doi: 10.1007/s10439-016-1583-9
130. Zhao F, Yao D, Guo R, et al. Composites of polymer hydrogels and nanoparticulate systems for biomedical and pharmaceutical applications. Nanomaterials. 2015;5(4):2054–2130. doi: 10.3390/nano5042054
131. Bastiancich C, Bianco J, Vanvarenberg K, et al. Injectable nanomedicine hydrogel for local chemotherapy of glioblastoma after surgical resection. J Control Release. 2017;264:45–54. doi: 10.1016/j.jconrel.2017.08.019
132. Wang M, Bergès R, Malfanti A, et al. Local delivery of doxorubicin prodrug via lipid nanocapsule–based hydrogel for the treatment of glioblastoma. Drug Deliv Transl Res. 2024;14(12):3322–3338. doi: 10.1007/s13346-023-01456-y
133. Bastiancich C, Bozzato E, Luyten U, et al. Drug combination using an injectable nanomedicine hydrogel for glioblastoma treatment. Int J Pharm. 2019;559:220–227. doi: 10.1016/j.ijpharm.2019.01.042
134. Bozzato E, Tsakiris N, Paquot A, et al. Dual-drug loaded nanomedicine hydrogel as a therapeutic platform to target both residual glioblastoma and glioma stem cells. Int J Pharm. 2022;628:122341. doi: 10.1016/j.ijpharm.2022.122341
135. Gazaille C, Bozzato E, Madadian-Bozorg N, et al. Glioblastoma-targeted, local and sustained drug delivery system based on an unconventional lipid nanocapsule hydrogel. Biomater Adv. 2023;153:213549. doi: 10.1016/j.bioadv.2023.213549
136. Zhao Z, Shen J, Zhang L, et al. Injectable postoperative enzyme-responsive hydrogels for reversing temozolomide resistance and reducing local recurrence after glioma operation. Biomater Sci. 2020;8(19):5306–5316. doi: 10.1039/D0BM00338G
137. Cao X, Li S, Chen W, et al. Multifunctional hybrid hydrogel system enhanced the therapeutic efficacy of treatments for postoperative glioma. ACS Appl Mater Interfaces. 2022;14(24):27623–27633. doi: 10.1021/acsami.2c05147
138. Fourniols T, Randolph LD, Staub A, et al. Temozolomide-loaded photopolymerizable PEG-DMA-based hydrogel for the treatment of glioblastoma. J Control Release. 2015;210:95–104. doi: 10.1016/j.jconrel.2015.05.272
139. Lin F-W, Chen P-Y, Wei K-C, et al. Rapid in situ MRI traceable gel-forming dual-drug delivery for synergistic therapy of brain tumor. Theranostics. 2017;7(9):2524. doi: 10.7150/thno.19856
140. Zhang R, Ye Y, Wu J, et al. Immunostimulant in situ fibrin gel for post-operative glioblastoma treatment by macrophage

reprogramming and photo–chemo-immunotherapy. ACS Appl Mater Interfaces. 2023;15(14):17627–17640. doi: 10.1021/acsami.3c00468
141. Jia M, Zhou X, Li P, et al. An injectable biomimetic hydrogel adapting brain tissue mechanical strength for postoperative treatment of glioblastoma without anti-tumor drugs participation. J Control Release. 2024;373:699–712. doi: 10.1016/j.jconrel.2024.07.068
142. Wang F, Huang Q, Su H, et al. Self-assembling paclitaxel-mediated stimulation of tumor-associated macrophages for postoperative treatment of glioblastoma. Proc Natl Acad Sci USA. 2023;120(18):e2204621120. doi: 10.1073/pnas.2204621120
143. Moore KM, Murthy AB, Graham-Gurysh EG, et al. Polymeric biomaterial scaffolds for tumoricidal stem cell glioblastoma therapy. ACS Biomater Sci Eng. 2020;6(7):3762–3777. doi: 10.1021/acsbiomaterials.0c00477
144. Damus BJ, Amaeze NR, Yoo E, et al. Ethoxy Acetalated dextran-based biomaterials for therapeutic applications. Polymers. 2024;16(19):2756. doi: 10.3390/polym16192756
145. Graham-Gurysh E, Moore KM, Satterlee AB, et al. Sustained delivery of doxorubicin via acetalated dextran scaffold prevents glioblastoma recurrence after surgical resection. Mol Pharm. 2018;15(3):1309–1318. doi: 10.1021/acs.molpharmaceut.7b01114
146. Graham-Gurysh EG, Moore KM, Schorzman AN, et al. Tumor responsive and tunable polymeric platform for optimized delivery of paclitaxel to treat glioblastoma. ACS Appl Mater Interfaces. 2020;12(17):19345–19356. doi: 10.1021/acsami.0c04102
147. Graham-Gurysh EG, Murthy AB, Moore KM, et al. Synergistic drug combinations for a precision medicine approach to interstitial glioblastoma therapy. J Control Release. 2020;323:282–292. doi: 10.1016/j.jconrel.2020.04.028
148. Serra R, Smith SJ, Rowlinson J, et al. Neurosurgical application of olaparib from a thermo-responsive paste potentiates DNA damage to prolong survival in malignant glioma. Br J Cancer. 2024;131(11):1858–1868. doi: 10.1038/s41416-024-02878-2
149. McCrorie P, Mistry J, Taresco V, et al. Etoposide and olaparib polymer-coated nanoparticles within a bioadhesive sprayable hydrogel for post-surgical localised delivery to brain tumours. Eur J Pharm Biopharmaceutics. 2020;157:108–120. doi: 10.1016/j.ejpb.2020.10.005
150. Grayson ACR, Choi IS, Tyler BM, et al. Multi-pulse drug delivery from a resorbable polymeric microchip device. Nat Mater. 2003;2(11):767–772. doi: 10.1038/nmat998
151. Gawley M, Almond L, Daniel S, et al. Development and in vivo evaluation of irinotecan-loaded drug eluting seeds (iDES) for the localised treatment of recurrent glioblastoma multiforme. J Control Release. 2020;324:1–16. doi: 10.1016/j.jconrel.2020.05.012
152. Lee J, Cho HR, Cha GD, et al. Flexible, sticky, and biodegradable wireless device for drug delivery to brain tumors. Nat Commun. 2019;10(1):5205. doi: 10.1038/s41467-019-13198-y
•• **In this work the authors designed a patch integrated with wireless electronics for controlled intracranial drug delivery through mild-thermic actuation. Moreover, an intheresting canine model of GBM, has been used, overcoming limitations associated with rodent models.**
153. Di Mascolo D, Palange AL, Primavera R, et al. Conformable hierarchically engineered polymeric micromeshes enabling combinatorial therapies in brain tumours. Nat Nanotechnol. 2021;16(7):820–829. doi: 10.1038/s41565-021-00879-3
154. Di Mascolo D, Guerriero I, Pesce C, et al. μMESH-enabled sustained delivery of molecular and nanoformulated drugs for glioblastoma treatment. ACS Nano. 2023;17(15):14572–14585. doi: 10.1021/acsnano.3c01574
155. Holla Nd C, Numata K, Rnjak-Kovacina J, et al. The biomedical use of silk: past, present, future. Adv Healthcare Mater. 2019;8(1):1800465. doi: 10.1002/adhm.201800465
156. Wang Z, Yang Z, Jiang J, et al. Silk microneedle patch capable of on-demand multidrug delivery to the brain for glioblastoma treatment. Adv Mater. 2022;34(1):2106606. doi: 10.1002/adma.202106606
157. Narsinh KH, Kumar K, Bankiewicz K, et al. A phase I study of convection-enhanced delivery (CED) of liposomal-irinotecan using real-time magnetic resonance imaging in patients with recurrent high-grade glioma. J Neurooncol. 2025;172(1):219–227. doi: 10.1007/s11060-024-04904-y
158. Mueller S, Kline C, Stoller S, et al. PNOC015: repeated convection-enhanced delivery of MTX110 (aqueous panobinostat) in children with newly diagnosed diffuse intrinsic pontine glioma. Neuro Oncol. 2023;25(11):2074–2086. doi: 10.1093/neuonc/noad105
159. Brenner AJ, Patel T, Bao A, et al. Convection enhanced delivery of rhenium (186Re) Obisbemeda (186RNL) in recurrent glioma: a multicenter, single arm, phase 1 clinical trial. Nat Commun. 2025;16(1):2079. doi: 10.1038/s41467-025-57263-1
160. Grauer O, Jaber M, Hess K, et al. Combined intracavitary thermotherapy with iron oxide nanoparticles and radiotherapy as local treatment modality in recurrent glioblastoma patients. J Neurooncol. 2019;141(1):83–94. doi: 10.1007/s11060-018-03005-x
161. Peruzzi P, Dominas C, Fell G, et al. Intratumoral drug-releasing microdevices allow in situ high-throughput pharmaco phenotyping in patients with gliomas. Sci Transl Med. 2023;15(712):eadi0069. doi: 10.1126/scitranslmed.adi0069
162. Pozzi S, Scomparin A, Dangoor SI, et al. Meet me halfway: are in vitro 3D cancer models on the way to replace in vivo models for nanomedicine development? Adv Drug Deliv Rev. 2021;175:113760. doi: 10.1016/j.addr.2021.04.001
163. Haddad AF, Young JS, Amara D, et al. Mouse models of glioblastoma for the evaluation of novel therapeutic strategies. neuro-Oncol Adv. 2021;3(1):vdab100. doi: 10.1093/noajnl/vdab100
164. Mnich K, Lhomond S, Wallace E, et al. Improving glioblastoma treatment with imaging, radiotherapy, drug delivery, and therapeutic systems. Device. 2025;3(2):100685. doi: 10.1016/j.device.2024.100685
165. Liu Y, Strawderman MS, Warren KT, et al. Clinical efficacy of tumor treating fields for newly diagnosed glioblastoma. Anticancer Res. 2020;40(10):5801–5806. doi: 10.21873/anticanres.14597
166. Pesaresi A, La Cava P, Bonada M, et al. Combined fluorescence-guided surgery with 5-aminolevulinic acid and fluorescein in glioblastoma: technical description and report of 100 cases. Cancers (Basel). 2024;16(16):2771. doi: 10.3390/cancers16162771
167. Kudruk S, Forsyth CM, Dion MZ, et al. Multimodal neuro-nanotechnology: challenging the existing paradigm in glioblastoma therapy. Proc Natl Acad Sci USA. 2024;121(8):e2306973121. doi: 10.1073/pnas.2306973121
168. Đorđević S, Gonzalez MM, Conejos-Sánchez I, et al. Current hurdles to the translation of nanomedicines from bench to the clinic. Drug Deliv Transl Res. 2022;12(3):500–525.